博士論文 （要約）

The metabolism of thiosulfate in *Hydrogenobacter thermophilus* TK-6

（*Hydrogenobacter thermophilus* TK-6 の チオ硫酸代謝）

小倉　一将

Table of contents

Preface and acknowledgment

この研究は東京大学大学院農学生命科学研究科応用生命工学専攻の応用微生物学研究室において、石井正治教授のご指導のもと行われました。

私の研究において、常に熱心なご指導と数々の有益なアドバイスを下さった、石井正治教授に深く感謝致します。自由に研究する環境を与えて下さり、時に温かく、時に厳しく研究を見守って頂いたおかげで、私は研究者として大きく成長できました。

微生物に関する深い造詣と、的確なアドバイスで常にサポートしていただいた、新井博之准教授に感謝致します。新井先生の鋭いコメントは、いつも私に深く考えるきっかけを作って下さいました。

応用微生物学研究室の卒業生として、また 2017 年 9 月からは助教として、私の研究を支えてくださった、亀谷将史助教に感謝致します。

突然の留学の申し出を快くお受け下さり、また留学期間中も多くのサポートを下さった、ドイツ、ボン大学の Dr. Prof. Christiane Dahl に感謝致します。Dahl 先生のご指導がなければ、私は硫黄代謝にここまで興味を持つことはできませんでした。

H. thermophilus における硫黄代謝の先駆者である、三本木至宏教授（広島大学大学院)、石崎優さんを始め、*H. thermophilus* の知識を積み上げてきて下さった先輩方に感謝致します。

応用微生物学研究室で共に研究を行った、同輩、後輩に感謝致します。特に、同じ *H. thermophilus* を研究対象とした、Dr. Kim KeugTae、加藤真美さん、井上達也さん、小林あずささん、河野岳さん、中山宗一郎さん、王静雨さん、浅野泰英さんとは、多くの時間を共に過ごし、いつも私に新鮮な驚きとインスピレーションを与えて下さいました。

2016 年から、応用微生物学研究室に新たな風を吹き込んで下さった、CO_2 資源化研究所の皆様に感謝致します。

そして、私の意思を尊重し、研究の道へ進むことを許して下さった、父・健司、母・恵美子には特に深く感謝致します。また実家を離れても顔を合わせれば変わらぬ距離感で接してくれる、妹・光莉、弟・健太郎にも感謝致します。

最後に、生命の面白さ、奥深さを教えて頂いた、*Hydrogenobacter thermophilus* TK-6 に感謝を申し上げます。

General introduction

Sulfur and life

Sulfur is the 16th element in the periodic table of elements. Sulfur atoms can take various oxidation states on Earth: the most reduced form, sulfide (S^{2-}), and the most oxidized form, sulfate (S^{6+}) (1). This element is an essential element for life as well as carbon, hydrogen, oxygen and nitrogen. At the cellular level, sulfur is needed for synthesis for amino acids, cysteine and methionine, and is found in the co-factors, thiamine pyrophosphate, coenzyme A and biotin as well as α-lipoic acid (2). Also, reduced sulfur compounds, such as sulfide, sulfur, and thiosulfate are important electron donors and energy sources in some bacteria and archaea. Chemolithoautotrophs utilize the energy for various cellular metabolisms including the fixation of CO_2.

Hydrogenobacter thermophilus

Hydrogenobacter thermophilus TK-6 (IAM 12695, DSMZ 6534) is a thermophilic and chemolithoautotrophic hydrogen-oxidizing bacterium, isolated from a hot spring in Izu, Japan in 1980 (3). This bacterium belongs to the order *Aquificales*, which is the deepest branch of the domain Bacteria in the 16S rRNA phylogenetic analysis (4). Many interesting features have been revealed from this bacterium, such as a unique quinone (5), cytochrome c_{552} (6), hydrogenase (7), carbon fixation (8-12), nitrogen assimilation (13-15), amino acid metabolism (13-15) and oxygen tolerance (18). The physiological properties of this bacterium are summarized in table 0-1.

Table 0-1 Physiological properties of *H. thermophilus*

Properties	Description
Cell shape[*1]	Long straight rod, 2.0-3.0 x 0.3 μm
Gram reaction[*1]	Negative
Motility[*1]	Negative
GC content (mol%)[*2]	44.0 mol%
Cellular fatty acid[*3]	$C_{18:0}$, $C_{20:1}$
Phospholipid[*4]	Aminophospholipid (PX), PI, PG
Quinone[*5]	Methionaquinone
Cytochrome[*1,6]	b_{560}, c_{552}, o
Growth temperature[*3]	Optimum: 70-75°C
Electron donor[*1, 7]	H_2, $Na_2S_2O_3$
Terminal electron acceptor[*1, 7, 8, 9]	O_2, NO_3^-, Fe^{3+}, S
Carbon source[*1]	CO_2
Nitrogen source[*3]	NH_4^+, NO_3^-
Sulfur source[*1, 7]	$Na_2S_2O_3$, SO_4^{2-}
CO_2-fixation pathway[*10]	Reductive TCA cycle

[*1](3), [*2](19), [*3](20), [*4](24), [*5](5), [*6](6), [*7](21), [*8](22), [*9](23)

Sulfur metabolism of *H. thermophilus*

H. thermophilus utilizes sulfate and thiosulfate as a sulfur source during growth. Also, thiosulfate can be utilized as a sole electron donor as well as hydrogen. When *H. thermophilus* is grown with thiosulfate as the sole electron source, particles derived from sulfur species are found in the culture medium with decrease of pH. The amount of sulfur globules decreases by further cultivation. From these results and genomic information of *H. thermophilus*, sulfur metabolism of *H. thermophilus* was proposed as follows.

(1) Oxidation of thiosulfate

There are two different pathways for thiosulfate oxidation in the domain Bacteria. One is the sulfur oxidation (sox) system, and another is the S4 compound-intermediate (S4I) pathway. In *H. thermophilus*, there is a gene set encoding proteins of sox system (*soxY*, *Z*, *A1*, *A2*, *X*, *B*), but no gene encoding proteins of S4I pathway have been identified (25). The scheme of the sox system is shown in Fig. 0-1. In the sox system, multiple proteins present in the periplasm catalyze the reactions. First, thiosulfate is bound to a thiol group of SoxY, in which two electrons-oxidation is catalyzed by SoxAX. SoxY-bound thiosulfonate is then hydrolyzed by SoxB, generating SoxY-S-SH, sulfate, and two protons. Thiol group of SoxY-S-SH is cleaved, and insoluble sulfur species are released (this mechanism is still an enigma). Thus, the sulfane sulfur (sulfur atom forming covalent bond only with another sulfur atom) moiety and the $-SO_3$ group of thiosulfate are oxidized to insoluble sulfur species and sulfate, respectively, via the sox system.

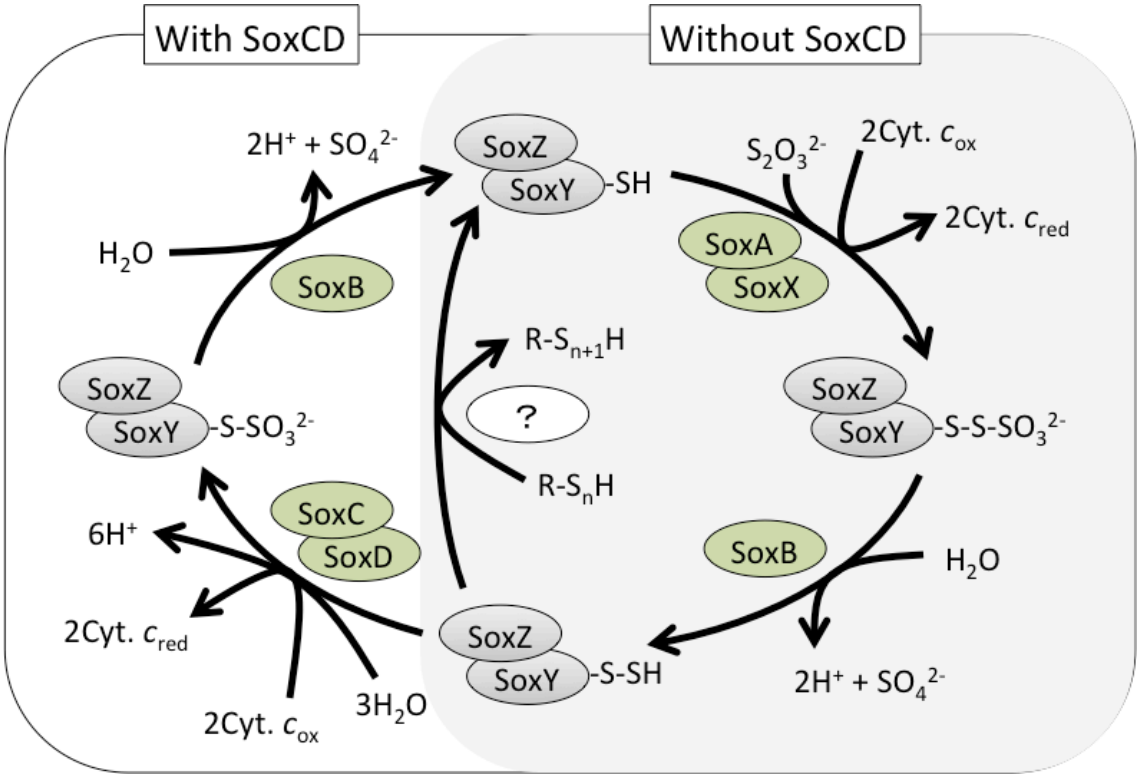

Fig. 0-1 Scheme of thiosulfate oxidation in sox system. Only right catalytic cycle is operated without SoxCD, whereas both left and right catalytic cycles are operated in the presence of SoxCD. *H. thermophilus* has a sox system lacking SoxCD. Cyt. c_{ox}, oxidized cytochrome *c*; Cyt. c_{red}, reduced cytochrome *c*.

(2) Oxidation of insoluble sulfur species

Oxidation of insoluble sulfur species is considered to occur in the cytoplasm while the mechanism of its transporting system is unknown. It is speculated that insoluble sulfur species are oxidized to sulfate by two sequential enzymes: heterodisulfide reductase-like protein (HdrAB1B2C1C2) and SreABC (HTH_1746, 1741, and 1740) (26, 27). However, detailed physiological analysis has not been performed. A part of insoluble sulfur species is converted to cysteine by CysK (HTH_0951). Various sulfur-containing compounds are synthesized using –SH group of cysteine.

(3) Sulfate assimilation

When *H. thermophilus* is cultivated using sulfate as a sulfur source, assimilatory sulfate reduction (ASR) pathway is used to assimilate sulfate. The gene set of ASR pathway is coded in HTH_0442-0449, and the sulfide produced in this pathway is converted to cysteine by CysK (Fig. 0-2, Table 0-2). As expression levels of this pathway are repressed when thiosulfate exists in culture medium, it is suggested that *H. thermophilus* preferentially uses thiosulfate than sulfate as a sulfur source (28).

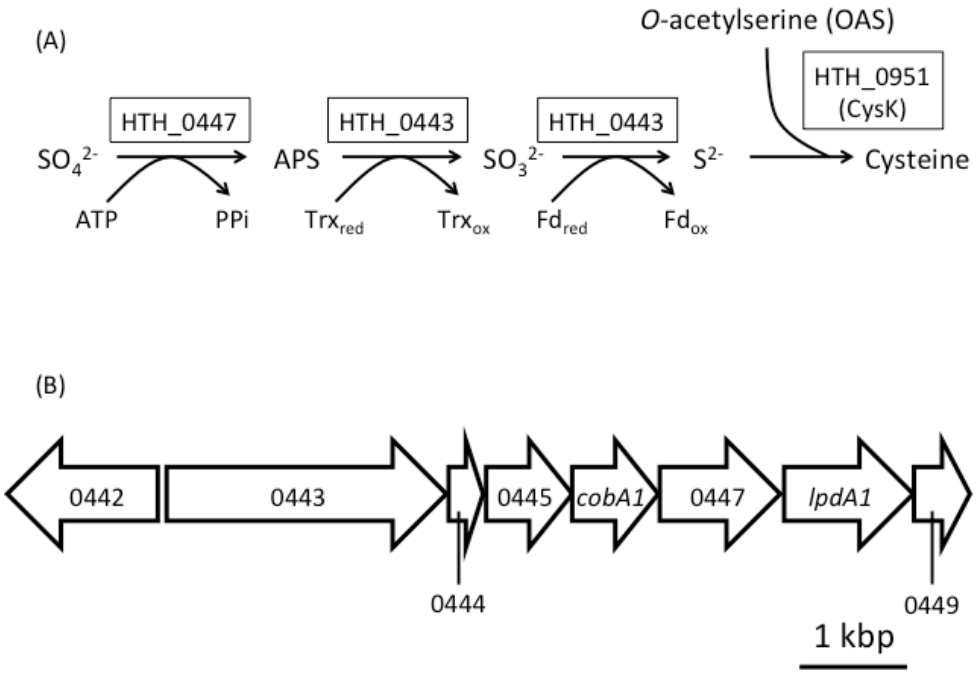

Fig. 0-2 The assimilatory sulfate reduction (ASR) pathway. (A) A metabolic pathway of the assimilatory sulfate reduction. APS, Adenosine-5'-phosphosulfate; Trx_{red}, reduced thioredoxin; Trx_{ox}, oxidized thioredoxin; Fd_{red}, reduced ferredoxin; Fd_{ox}, oxidized ferredoxin. (B) Gene map of HTH_0442-0449 in *H. thermophilus*. Predicted function of each gene is shown in Table 0-2.

Table 0-2 General information of HTH_0442-0449 in *H. thermophilus*.

Locus tag	Gene name	Predicted function
HTH_0442		σ54 dependent transcriptional regulator
HTH_0443		Ferredoxin-sulfite reductase and phosphoadenosine phosphosulfate reductase fusion protein
HTH_0444		Hypothetical protein
HTH_0445		Sulfite transporter
HTH_0446	*cobA1*	Uroporphyrinogen-III methyltransferase
HTH_0447		sulfate adenylyl transferase
HTH_0448	*lpdA1*	dihydrolipoamide dehydrogenase
HTH_0449		Hypothetical protein

Objectives of this study

I am particularly interested in energy metabolism which uses sulfur. Studying on the metabolism of inorganic sulfur compounds is important for considering the metabolism of early life (29). However, there are few reports on the sulfur metabolism of chemolithoautotrophs or organisms located in a deepest branch of the phylogenetic tree (e.g. archaea and old bacteria), compared to those of the other organisms (e.g. phototrophic bacteria and iron-oxidizing bacteria). Therefore, investigating sulfur energy metabolism of chemolithoautotroph is essential for understanding initial metabolism of life.

H. thermophilus was used as a model organism in my research. This bacterium is the chemolithoautotroph, which is suggested to be located in the deepest branch of domain Bacteria by 16S rRNA phylogenetic analysis. In addition, *H. thermophilus* has great advantage to study sulfur metabolism. First, omics data, such as genome, transcriptome, and metabolome are available. These are powerful tools for looking over the metabolism. Secondly, genetic manipulation techniques of *H. thermophilus* are established. It is possible to predict the function of the gene *in vivo* by analyzing the gene-disrupted mutant. Lastly, various novel enzymes and metabolic pathways have been found in this bacterium. These are why I chose *H. thermophilus* for the study.

From the above background, the objective of this study is to clarify the full picture of sulfur energy metabolism in *H. thermophilus*. So far, a part of thiosulfate oxidation pathway was predicted from the genome data of *H. thermophilus*, and some enzymes have been studied (25, 30). In this study, further analyses about genes involved in the thiosulfate oxidation pathway were performed in chapter 1 and chapter 2. In chapter 3, sulfur globule produced by *H. thermophilus* was analyzed. Finally, I proposed a revised model for thiosulfate oxidation pathway in *H. thermophilus*.

Chapter 1 Sulfur-oxidizing enzyme

1-1 Physiological analysis of sulfur-oxidizing gene

1-1-0 Introduction

Inorganic sulfur compounds exist in various environments and these are metabolized by sulfur-oxidizing prokaryotes. Although these microbes play an important role in the sulfur cycle in the environment, there are many unknown parts about the prokaryotic sulfur energy pathway.

Metabolic pathways of sulfur oxidation are very diverse, so that no universal mechanism for the oxidation of reduced sulfur compounds exist. The most studied sulfur oxidation metabolism is the Dsr pathway (Fig. 1-1(A)) (1). This pathway uses the reverse reaction of sulfite reductase, an enzyme involved in the dissimilatory sulfite reduction pathway. In this pathway, sulfur imported into the cytoplasm is delivered to DsrC, which is the final acceptor mediated by a rhodanese and other sulfur carriers. DsrC is a substrate for sulfite reductase (DsrAB). The –SH group transferred to DsrC is oxidized to an $–SO_3$ group by sulfite reductase (DsrAB), followed by the release of sulfite.

On the other hand, some chemotrophic and phototrophic sulfur-oxidizing bacteria, including *H. thermophilus*, do not have the Dsr pathway. Transcriptional analyses in several archaea and bacteria suggested that a heterodisulfide reductase (Hdr)-like enzyme mediates sulfur oxidation (Fig. 1-1(B)) (2, 3). Hdr was originally characterized in methanogen and catalyzes the reduction of heterodisulfide of CoM-S-S-CoB produced by the final step of methanogenesis (4). It is believed that Hdr in sulfur-oxidizing bacteria performs a completely different function from that in methanogen and oxidizes sulfur to sulfite instead of the Dsr pathway. Recently, localization and complex structure of Hdr were investigated in *Aquifex aeolicus* which is a closely related species of *H. thermophilus* (5). It is indicated that the Hdr in *A. aeolicus* is associated to the membrane in the cell and consists of at least five subunits (HdrAB1B2C1C2). Although the enzymatic feature of Hdr gradually becomes revealed, there is no data on its physiological properties. Therefore, I focused on *hdr* in *H. thermophilus* and aimed to clarify its function *in vivo* by phenotypic profiling and transcriptional analysis of a gene-disrupted mutant strain.

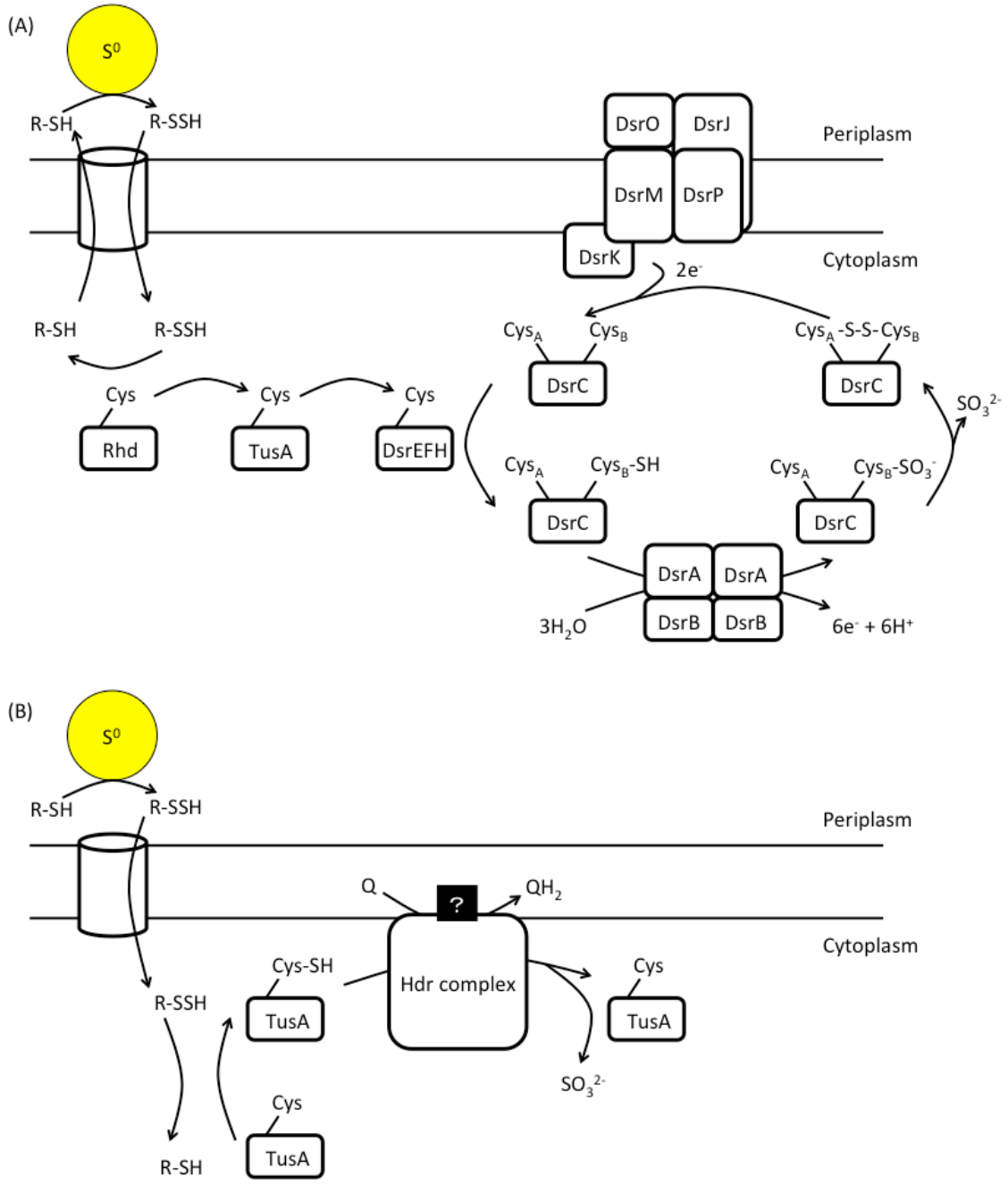

Fig. 1-1 Model for sulfur oxidation via the Dsr pathway and the Hdr pathway. (A) The Dsr pathway in *Allochromatium vinosum*. (B) The proposed Hdr pathway in *A. aeolicus*. Rhd (Rhodanese), TusA and DsrEFH function as sulfur carriers. DsrC is the substrate for sulfite reductase (DsrAB). DsrAB and Hdr complex oxidize persulfide in the substrate protein. DsrJKMOP complex reduces the oxidized form of DsrC. R-SH denotes a low molecular weight organic persulfide, which is presumed to transfer sulfur into the cytoplasm, but this mechanism is not yet clarified.

1-1-1 Materials and methods

Bacterial strain and growth condition. *H. thermophilus* TK-6 (IAM 12695, DSMZ 6534) was cultivated at 70°C in a sulfate-limited inorganic medium in a 100-mL vial (Table 1-1) ((6), with a little modification). Note that this sulfate-limited medium contains about 50 μM sulfate, which is sufficient to support the growth of *H. thermophilus* (Fig. 1-2). Hydrogen or sodium thiosulfate was added as an energy source. For the thiosulfate-oxidizing growth, 10 mM sodium thiosulfate was supplied to the medium. The gas phase in the vial was replaced with gas mixtures of H_2:O_2:CO_2 (75:10:15) and N_2:O_2:CO_2 (75:10:15) for the hydrogen-oxidizing condition and the thiosulfate-oxidizing condition, respectively. For the growth test, the preculture was inoculated into 20 mL of sulfate-limited inorganic medium in 100-mL vial. The cell number, pH, and concentration of sulfur compounds (see below) were measured at intervals of 3 hours. The cell number was determined by a counting chamber (AS ONE). The initial cell number was adjusted to 5.0 x 10^7 cells/mL.

Table 1-1 Sulfate-limited inorganic medium for the cultivation of *H. thermophilus*

NH_4Cl*1	2.4 g		
KH_2PO_4	1 g	*Trace element solution	
K_2HPO_4	2 g	MoO_3	4 mg
$MgCl_2•6H_2O$*2	0.5 g	$ZnSO_4•7H_2O$	28 mg
NaCl	0.25 g	$CuSO_4•5H_2O$	2 mg
$CaCl_2$	0.03 g	H_3BO_3	4 mg
$FeSO_4•7H_2O$	14 mg	$MnSO_4•5H_2O$	4 mg
Trace element solution*	0.5 mL	$CoCl_2•6H_2O$	4 mg
Deionized water	1 L	Deionized water	1 L

*1 $(NH_4)_2SO_4$ used in conventional culture medium for *H. thermophilus* was replaced by NH_4Cl.

*2 $MgSO_4•7H_2O$ used in conventional culture medium for *H. thermophilus* was replaced by $MgCl_2•6H_2O$.

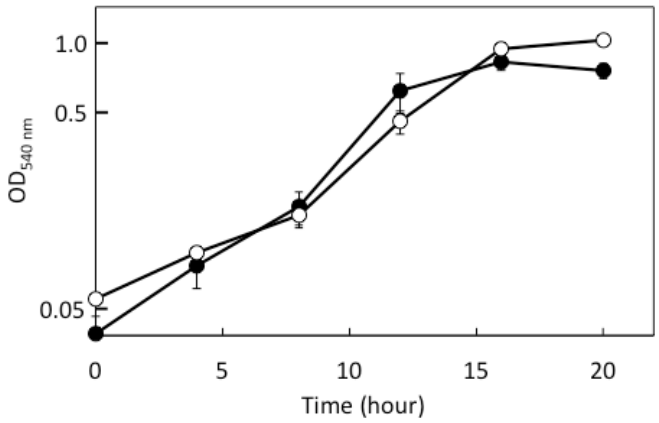

Fig. 1-2 Growth curves of wild type in conventional culture medium and sulfate-limited culture medium. Growth profile of *H. thermophilus* wild type under the aerobic (10% O_2) and the hydrogen-oxidizing (H_2:O_2:CO_2 = 75:10:15, v/v) condition in conventional and sulfate-limited culture medium was observed. Optical density at 540 nm was measured at intervals of four hours. Culture medium type: conventional culture medium (●) and sulfate-limited medium (○). Error bars show the standard deviation of each triplicate value.

Construction of a Δ*hdrA* mutant. A plasmid for gene disruption was constructed and used for mutant construction according to a homologous recombination method reported in a previous study (Fig. 1-3 and Table 1-2) (7). In brief, plasmid pEX18-dhdrA was constructed based on pEX18Ap vector and transformed to *Escherichia coli* S17-1. *H. thermophilus* and transformed *E. coli* S17-1 were co-incubated at 37°C for 24 hours to allow plasmid transfer by conjugation. After the incubation, recombinant the colonies of *H. thermophilus* were selected on plate medium containing kanamycin under gas phase of H_2:O_2:CO_2 (75:10:15) at 70°C. The disruption of the gene was confirmed by PCR. When the constructed mutant was cultivated, 50 μg/mL of kanamycin was supplied to the medium.

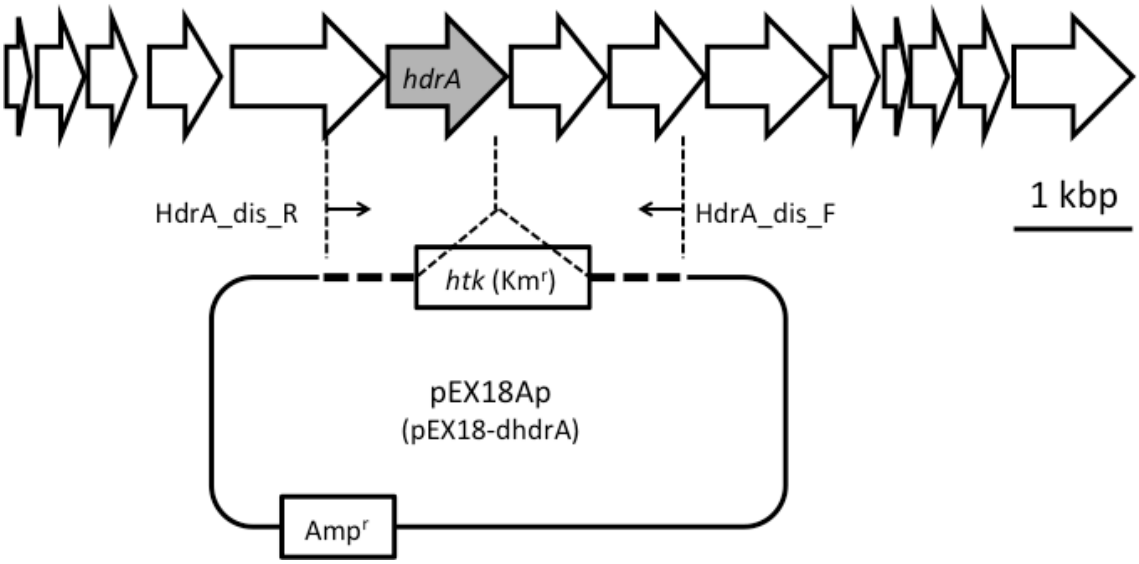

Fig. 1-3 Scheme for the construction of the plasmid. The gray arrow indicates *hdrA*, the targeted gene for disruption. The dashed lines in the plasmid indicate the regions that share identical sequences with the chromosomal DNA of *H. thermophilus*. The small arrows indicate the binding sites of the primers used for PCR (Table 1-2). *htk*, highly thermostable kanamycin resistance gene fused with promoter region of *H. thermophilus rpoD* gene; Km, kanamycin; Amp, ampicillin.

Table 1-2 List of primers used in chapter 1-1.

Primer	Sequence	Restriction site
HdrA_dis_F	TTGGGTACCTCCTCTACCAG	KpnI
HdrA_dis_R	TGGGCATGCTCCTCTTATGAAC	SphI

In the sequence, restriction sites are indicated by underline, and restriction enzymes are showed in the right column.

Detection of sulfur compounds. Thiosulfate, insoluble sulfur species and sulfate were determined by colorimetric or turbidometric methods. Sampled culture was separated to supernatant and pellet by centrifugation at 10,000 x *g* for 10 min. The supernatant was used for detection of thiosulfate and sulfate. The pellet was washed by deionized water and centrifuged at 10,000 x *g* for 10 min. Washed pellet was resuspended in 200 μL of distilled water and used for the detection of insoluble sulfur species.

Thiosulfate. Thiosulfate was determined via cyanolysis in the following system (8). A 650-μL of sample was mixed with 200 μL of 0.2 M sodium acetate (pH 4.8), 50μL of 0.2 M KCN, 50 μL of 40 mM $CuCl_2$ and 50 μL of $Fe(NO_3)_3$ reagent (15 g of $Fe(NO_3)_3$•$9H_2O$ and 17 mL of 65% (v/v) HNO_3 made up to 50 mL with deionized water). The absorbance of a ferric thiocyanate at 460 nm was measured.

Insoluble sulfur species. Insoluble sulfur species (elemental sulfur, polysulfide and polythionate) were determined via cyanolysis in the following system (9). A 200-μL sample was mixed with 100 μL of 0.2 M KCN. The mixture was boiled for 10 min at 100°C. After boiling, 650 μL of deionized water was added and centrifuged for 2 min at 10,000 x *g* to remove the pellet. A 50-μL $Fe(NO_3)_3$ reagent was mixed and the absorbance of a ferric thiocyanate at 460 nm was measured.

Sulfate. Sulfate was determined by the following turbidometric method (10). A 400-μL sample was mixed with 400 μL of 0.5 M trichloroacetic acid (TCA) and 200 μL of $BaCl_2$ reagent (0.49 g of $BaCl_2$•$2H_2O$ and 7.5 g of polyethylene glycol 6,000 were made up to 50 mL with water). The sample was incubated for 20 min with mixing at every 5 min. The turbidity of a $BaSO_4$ at 450 nm was measured.

RNA extraction. RNA extraction was performed toward four independent cultures. At first, *H. thermophilus* TK-6 was grown in 5 L of sulfate-limited inorganic medium under the hydrogen-oxidizing condition in a 10-L jar fermenter. After 6 hours cultivation, 10 mM sodium thiosulfate was added to the medium and the gas phase was changed to N_2:O_2:CO_2 (75:10:15, v/v). After 2 hours cultivation under the thiosulfate-oxidizing condition, 10 mL of the culture was sampled for RNA extraction. Sampled culture was immediately mixed with 10 mL of RNA protect (Quiagen, Hilden

Germany). Cells were collected by centrifugation for 10 min at 3,000 x *g*. RNA was extracted from the cell pellet by a hot-phenol method as described below. The cell pellet was resuspended in 800 μL of RNase-free Tris/EDTA buffer (pH8.0) containing 1 mg/mL lysozyme. The suspension was mixed with 80 μL of 10% SDS and incubated for 2 min at 65°C. Then, 88 μL of 1 M sodium acetate (pH 5.2) and 1 mL of water-saturated phenol were supplied to the solution. The mixture was incubated at 65°C for 6 min with inversion. The samples were centrifuged at 13,000 x *g* for 10 min at 4°C. The upper aqueous layer was mixed with 1 mL of phenol/chloroform/isoamylalcohol (25:24:1) and centrifuged at 13,000 x *g* for 10 min at 4°C. The upper aqueous layer was mixed with 1 mL of chloroform/isoamylalcohol (24:1) and centrifuged at 13,000 x *g* for 10 min at 4°C. The aqueous layer was the mixed with a 1/10 volume of 3 M sodium acetate (pH 5.2), a 1/10 volume of 1 mM EDTA, and 2 volume of cold ethanol and placed more than 30 min at -80°C. After incubation, the solution was centrifuged at 13,000 x *g* for 10 min at 4°C. The pellet was washed with cold 80% ethanol. After centrifugation at 13,000 x *g* for 10 min at 4°C, the liquid was completely removed and the pellet was dried. The pellet was resuspended in 80 μL of RNase-free water. To remove DNA, the solution was mixed with 10 μL of 10 x DNase buffer and 10 μL of DNase and incubated at 37°C for 1 hour. The treated sample was purified by using an RNeasy Mini kit (Quiagen) according to the manufacturer's instructions. The DNase treatment and subsequent purification were repeated twice. DNA and protein contamination, and RNA integrity number (RIN) were checked. At first, RNA samples were tested for genomic DNA contamination by PCR amplification of the *fdx1* gene (219 bp). Secondly, A_{260}/A_{280} ratio of the samples was measured to check the contamination of protein. Lastly, RIN score for the quality of total RNA was measured by using Agilent RNA 6000 Nano kit (Agilent technologies).

Microarray experiments and data analysis. A customized tiling array with 8 x 15K format for *H. thermophilus* was designed and manufactured by Agilent technology (USA) based on the genome sequence. A probe set consisting of 132,517 oligonucleotide covering the *H. thermophilus* genome was used. Also, 15 genes were

chosen and used as a control ensuring that there was no contamination during hybridization step. Quadruplicate RNA samples were converted to double-strand (ds)-cDNA and cRNA. Synthesis, labeling, and purification of ds-cDNA and cRNA were performed by following the instruction of one-color microarray-based gene expression analysis (Agilent technologies). Then, 600 ng of cRNA was applied to hybridization step by following the protocol of Agilent technologies and the arrays were scanned with SureScan Microarray Scanner (Agilent technologies). Agilent Feature Extraction Software 10.7 was used for the extraction of the probe signal intensities and processing of the data. Expression data were analyzed by R program version 3.2.1. (11). The data were normalized by median normalization. Hierarchical clustering between samples was performed and confirmed whether each strain forms clusters. The mean signal values of each probe set and fold changes between wild type and mutant were calculated. Genes that showed more than 3-fold differences with 95% confidence were considered significant.

1-1-2 Results and discussion

Physiology of *hdrA*.

To investigate the function of *hdrA in vivo*, the phenotype of *hdrA* disruptant (Δ*hdrA*) was observed. Δ*hdrA* showed comparable growth to wild type when it was cultivated under the hydrogen-oxidizing condition (Fig. 1-4). Δ*hdrA* was cultivated under the aerobic and the thiosulfate-oxidizing condition, and its cell growth and the concentration of the sulfur species (thiosulfate, insoluble sulfur species and sulfate) were determined over time (Fig. 1-5). Δ*hdrA* gave poor growth compared with wild type (Fig. 1-5 (A)). Although the consumption rate of thiosulfate did not change, the amount of sulfate accumulated in the culture medium was halved (Fig. 1-5 (B) and (C)). In sox system in the periplasm, sulfane sulfur moiety of thiosulfate is metabolized to insoluble sulfur species. These sulfur species are imported to the cytoplasm and further oxidized to sulfate. It is suggested that the amount of sulfate in Δ*hdrA* was about half of that in wild type because insoluble sulfur species were not oxidized. This is consistent with the fact that the change of pH in Δ*hdrA* was small compared with wild type (Fig. 1-5 (E)). Therefore, it is suggested that *hdrA* is responsible for the

oxidation of sulfur and plays an important role for energy acquisition *in vivo* under the thiosulfate-oxidizing condition. The insoluble sulfur species concentration in the culture of Δ*hdrA* was higher than that of wild type, and these remained in the culture even in the later phase of the cultivation (Fig. 1-5 (D)).

The calculated total sulfur amount in the culture medium significantly decreased with time in Δ*hdrA* (Fig. 1-5 (F)). In addition, despite *hdrA* disruption, the amount of insoluble sulfur species decreased in the later stage of the cultivation. *H. thermophilus* has a unique smell, and recent works in our laboratory revealed that a part of the smell component is derived from sulfur-containing compound (Nakayama, unpublished data). It is considerable that a part of the sulfur species generated by the thiosulfate oxidation is released into the gas phase.

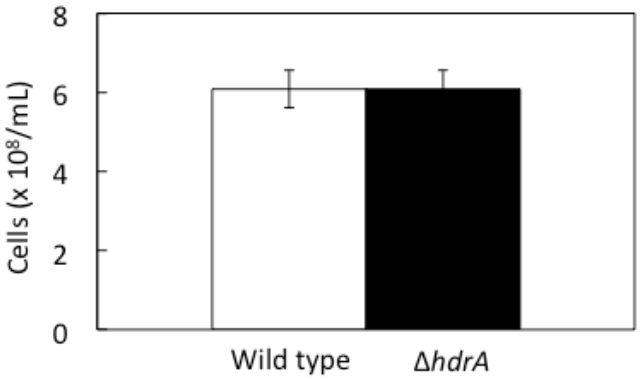

Fig. 1-4 The growth of wild type and Δ*hdrA* under the hydrogen-oxidizing condition. The cells after 12 hours cultivation under the aerobic and hydrogen-oxidizing condition were determined by a counting chamber (AS ONE). Open bar shows wild type and closed bar shows Δ*hdrA*. Error bars show the standard deviation of each triplicate value.

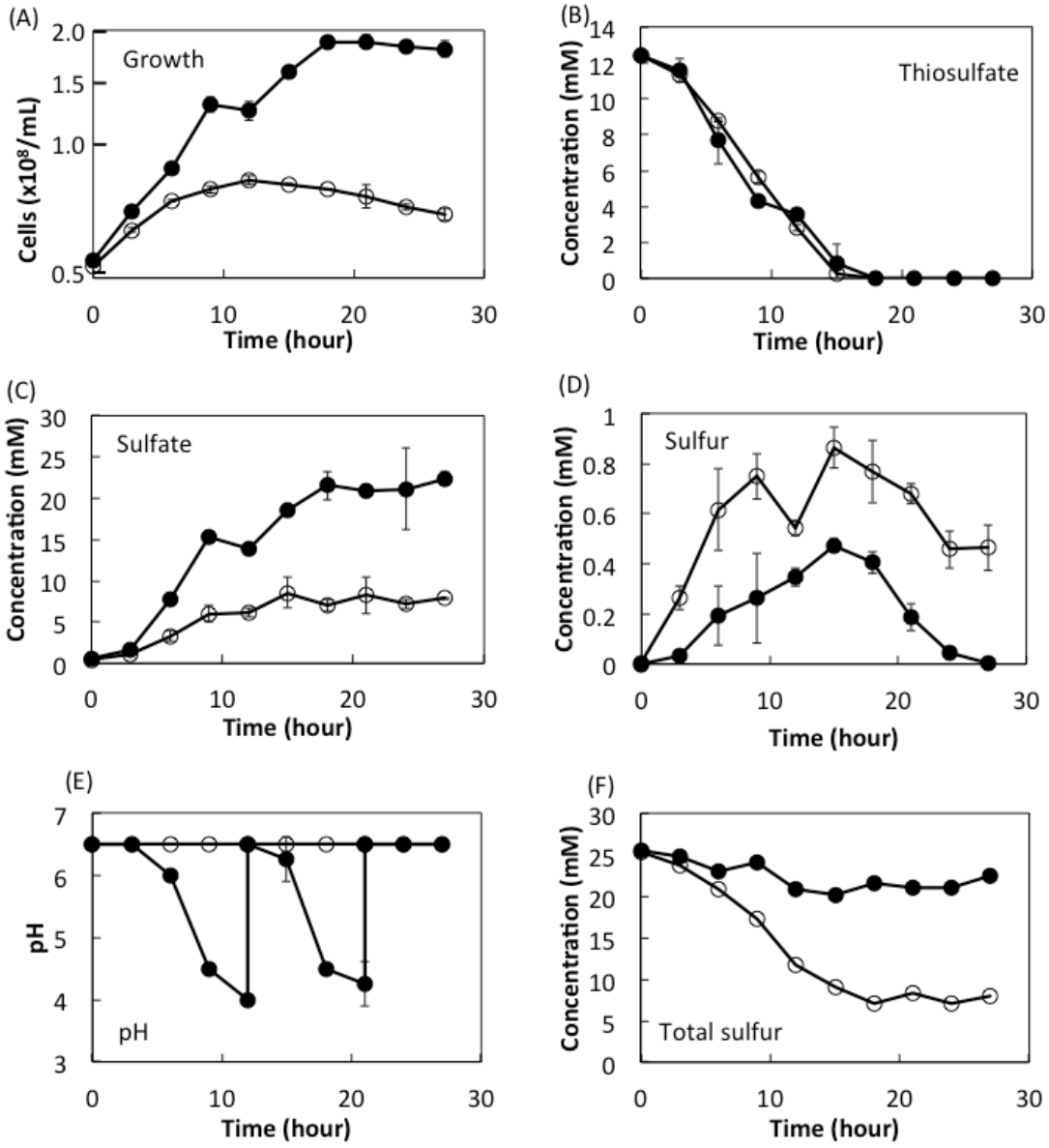

Fig. 1-5 Growth profiles of wild type and the *hdrA* mutant (Δ*hdrA*). Thiosulfate oxidation under the aerobic condition (10% O_2) by *H. thermophilus* wild type and Δ*hdrA* strains was observed. (A) Growth, (B) thiosulfate, (C) sulfate, (D) sulfur, (E) pH, and (F) total sulfur amount (calculated from (B) to (D)). *H. thermophilus* strains: WT (●), Δ*hdrA* (○). Error bars show the standard deviation of each duplicate value. Adjustment of pH was done by the addition of 1 M NaOH.

Transcriptional analysis.

To investigate the influence of disruption of Hdr gene on metabolism, microarray analysis was performed. Wild type and Δ*hdrA* were cultured under the thiosulfate-oxidizing condition, and gene expression levels were determined. A list of genes that showed more than 2-fold change with 95% confidence is shown in appendix.

I focused on the expression patterns of the genes for respiratory chain (Fig. 1-6). Although there was no significant difference in the expression level of NADH dehydrogenase (Fig. 1-6 (A)), the expression levels of bc_1 complex (*qcrABC*) and two out of four cytochrome *c* oxidases (*cox2* and *cyo*) were repressed (Fig. 1-6 (B, D, and F)). On the other hand, the expression levels of the other cytochrome *c* oxidases (*cox1* and *cox3*) did not change in Δ*hdrA* (Fig. 1-6 (C and E)). The former cytochrome *c* oxidases (*cox2* and *cyo*) are classified as a ba_3-type cytochrome *c* oxidase, and the latter cytochrome *c* oxidases (*cox1* and *cox3*) are classified as an aa_3-type cytochrome *c* oxidase. It is suggested that aa_3-type cytochrome *c* oxidases have more efficient proton pumping ability than ba_3-type cytochrome *c* oxidases (12, 13). Considering the poor growth of Δ*hdrA* under the thiosulfate-oxidizing condition (Fig. 1-5 (A)), it is reasonable that Δ*hdrA* promotes the use of aa_3-type cytochrome *c* oxidases by suppressing the expression levels of ba_3-type cytochrome *c* oxidases to utilize energy more efficiently.

The expression levels of genes for sox proteins (*soxYZA1A2XB*), which metabolize thiosulfate, tended to increase (Fig. 1-7 (A)), while there were no changes in the expression levels of *sreABC*, which is a sulfite-oxidizing enzyme (this enzyme will be discussed in chapter 2) (Fig. 1-7 (B)). Genes involved in the assimilatory sulfate reduction pathway are downregulated under the thiosulfate-oxidizing condition (14). This tendency did not change even in Δ*hdrA* (Fig. 1-7 (C)).

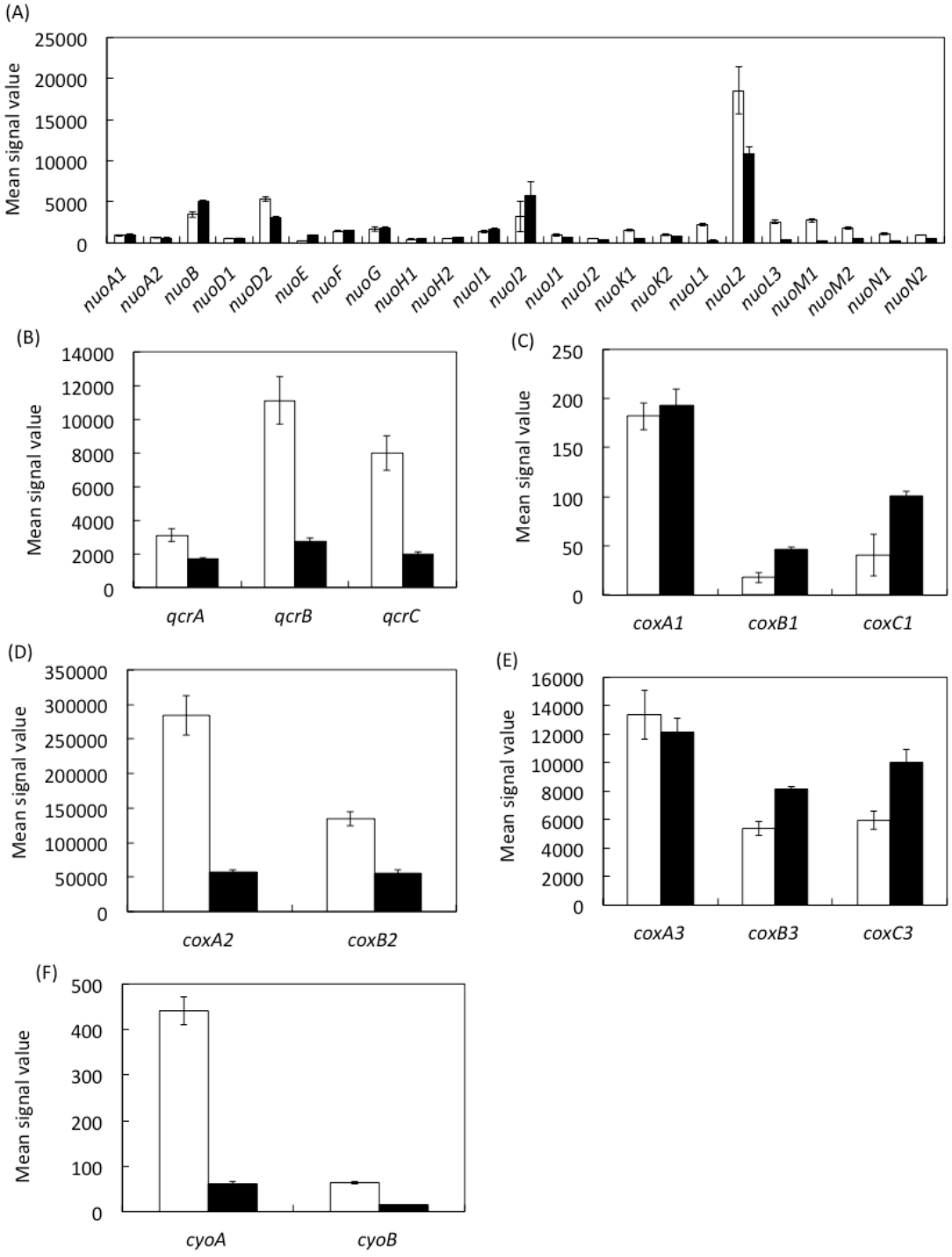

Fig. 1-6 Microarray expression profiles of the genes related to the respiratory chain. (A) Gene set for NADH dehydrogenase, (B) gene set for *bc*1 complex, (C) gene set for cytochrome *c* oxidase 1 (*cox1*), (D) gene set for cytochrome *c* oxidase 2 (*cox2*), (E) gene set for cytochrome *c* oxidase 3 (*cox3*), and (F) gene set for cytochrome *c* oxidase (*cyo*). Open bars denote wild type and closed bars denote Δ*hdrA*. The mean signal value is the average of the microarray signal value of a given gene.

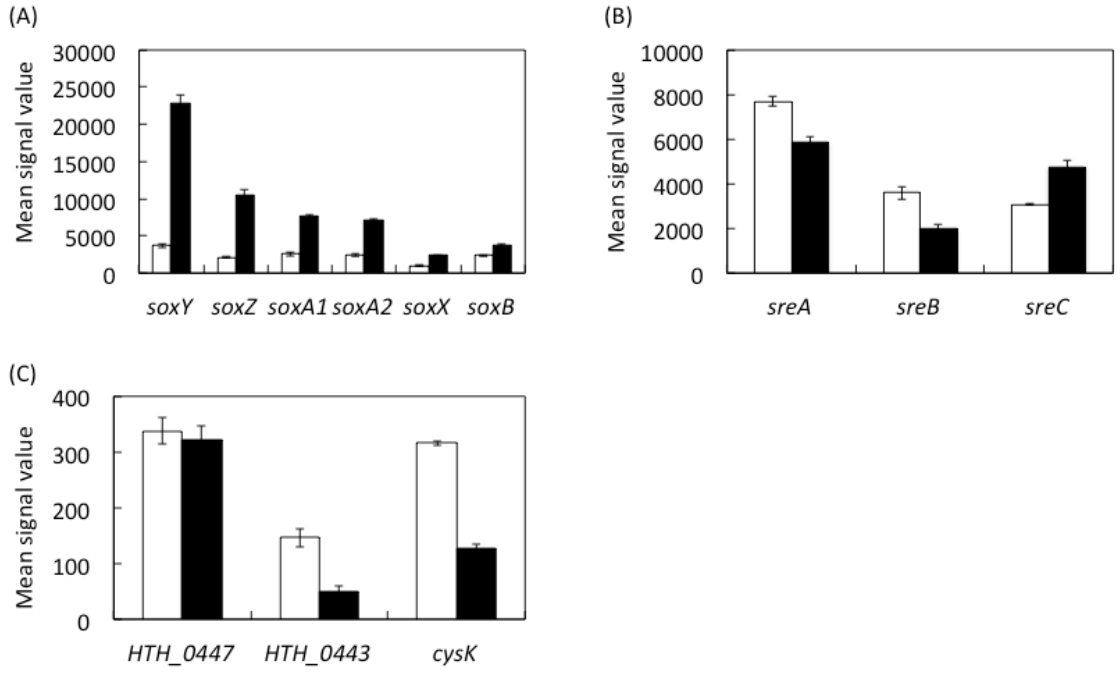

Fig. 1-7 Microarray expression profiles of the genes related to the sulfur metabolisms. (A) Gene set for thiosulfate oxidation proteins, (B) gene set for sulfite oxidoreductase, (C) gene set for assimilatory sulfate reduction (HTH_0447, sulfate adenylyl transferase; HTH_0443, APS reductase and sulfite reductase fusion protein; *cysK*, cysteine synthase). Open bars denote wild type and closed bars denote Δ*hdrA*. The mean signal value is the average of the microarray signal value of a given gene.

Interesting expression changes were observed in *hyn* cluster, which is one of the hydrogenases in *H. thermophilus* (Fig. 1-8). Expression levels of four genes including *hyn* were repressed in Δ*hdrA*. In *hyn* cluster, there are HTH_0093 and HTH_0094 genes between *hynS* and *hynL*. These genes are usually named as *isp1* and *isp2* in bacteria, encoding two proteins, Isp1 and Isp2 (15). Isp1 has the transmembrane region with a di-heme binding site (15). Isp2 is a soluble protein, which has the homology with heterodisulfide reductase D subunit (HdrD) of methanogen (15). In methanogen, HdrD catalyzes the reduction of heterodisulfide of CoM-S-S-CoB (16). HynLS hydrogenase makes a heterotetrameric complex associated with Isp1 and Isp2 in *Thiocapsa roseopersicina*, a purple sulfur bacterium (17). Since the expression levels of these genes were repressed by the disruption of *hdrA*, the proteins in *hyn* cluster may have a functional relationship with those in *hdr* cluster. The above results are summarized in the figure 1-9.

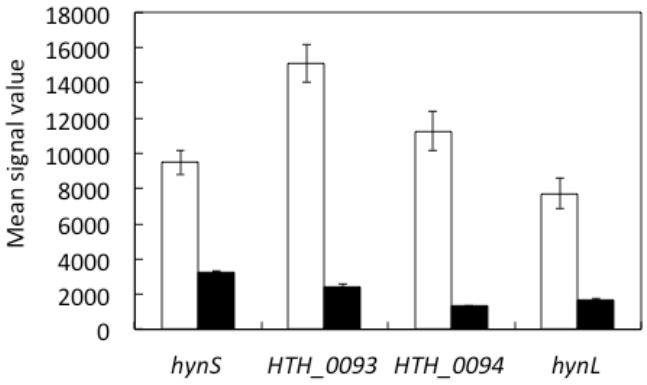

Fig. 1-8 Microarray expression profiles of the genes. Gene set for *hyn* cluster (*hynS*; HTH_0093, *isp1*; HTH_0094, *isp2*; *hynL*). Open bars denote wild type and closed bars denote Δ*hdrA*. The mean signal value is the average of the microarray signal value of a given gene.

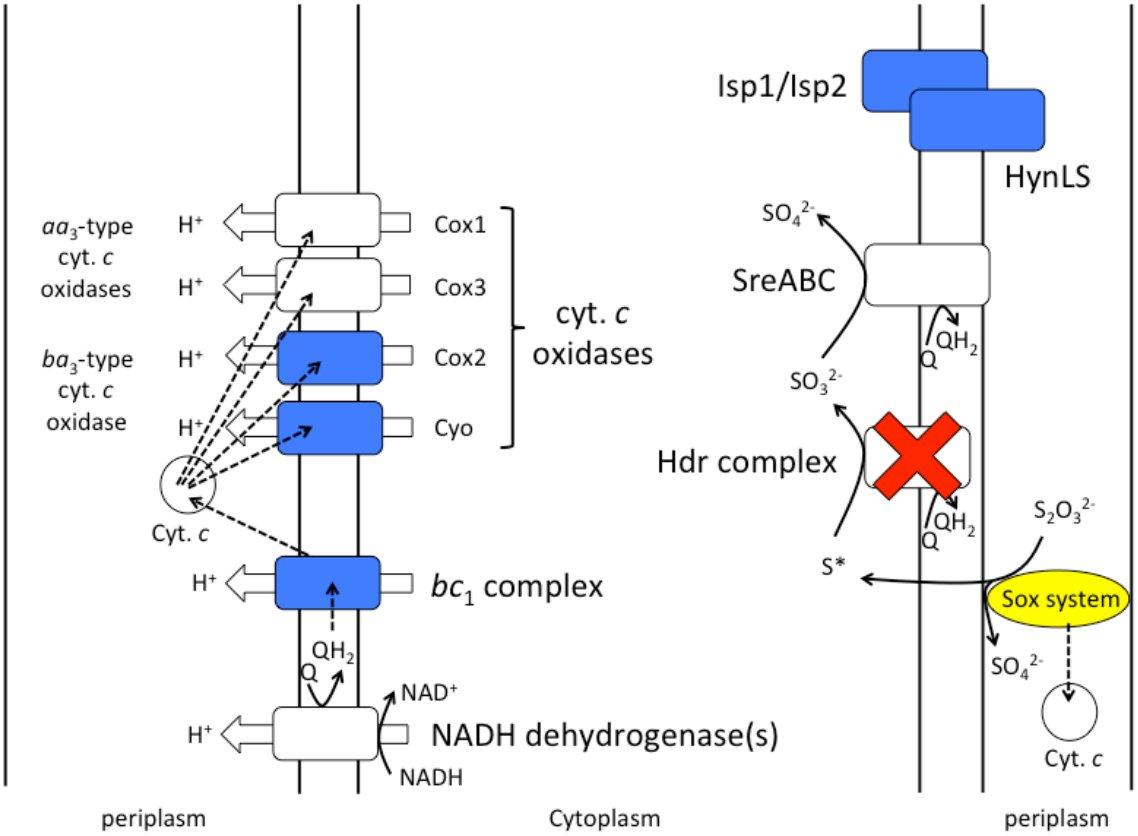

Fig. 1-9 Proposed model for metabolism in Δ*hdrA*. Genes for sox system, Hdr complex, Sulfite-oxidizing enzyme (SreABC), respiratory chain and Hyn hydrogenase complex are depicted. Up-regulated genes were colored in yellow, and down-regulated genes are colored in blue, respectively.

1-2 Functional analyses of glycine cleavage system genes present in the *hdr* gene cluster

1-2-0 Introduction

In *H. thermophilus*, the *hdr* gene cluster is a relatively large cluster, and some genes in it are conserved in other bacteria (Table 1-3). Genetic maps of *hdr* clusters of these bacteria are shown in Figure 1-10. In order to clarify enzymatic properties of Hdr enzyme in bacteria, it is important to investigate the function of the genes present in the *hdr* clusters. One or two genes conserved in the *hdr* cluster encode a homolog of glycine cleavage system H protein (GcvH) (1, 2), a member of a glycine degradation pathway (glycine cleavage system). Glycine cleavage system consists of three enzymes (P-protein, T-protein, and L-protein) and one carrier protein (H-protein) (3). The total reaction of this system is the following interconversion:

Gly + tetrahydrofolate (THF) + NAD^+ ⇄ 5,10-CH_2-THF + CO_2 + NH_3 + NADH + H^+

The *H. thermophilus* genome contains five genes encoding H-proteins homologs. Although constitutive expression of these genes was observed by transcriptional analysis (4), the glycine cleavage activity was not detected enzymatically (5). Furthermore, according to the annotation of Kyoto Encyclopedia of Genes and Genomes (KEGG: http://www.genome.jp/kegg/), some organisms belong to family *Aquificaceae*, lack at least one homolog of glycine cleavage protein. Then, what is the function of the GcvHs in *H. thermophilus*?

In methanogen, the Hdr enzyme oxidizes hydrogen, and reduces ferredoxin and CoM-S-S-CoB in the flavin-based electron bifurcating mechanism. Electron bifurcation is one of the mechanisms for energy conservation (6). It simultaneously couples exergonic and endergonic redox reactions to assist thermodynamically difficult steps. In the final step of methanogenesis in *Methanococcus maripaludis*, two electrons at the potential of hydrogen (-414 mV) undergo disproponation to reduce ferredoxin (-500 mV) and CoM-S-S-CoB (-150 mV) by Hdr complex (7). CoM-SH and CoB-SH created by this reaction are used again for methanogenesis. Thus, it is conceivable that the Hdr homolog in *H. thermophilus* exerts a similar bifurcated electron flow reacting with other substrates. As well as CoM-S-S-CoB, GcvH has a disulfide bond derived from a lipoyl group in its active site (3). I hypothesized that GcvH3 or GcvH4 (or both)

could be a substrate of bacterial Hdr complex (Fig. 1-11), but no experimental data were available for supporting this working hypothesis.

In this section, I focused on the GcvH proteins in the *hdr* cluster of *H. thermophilus*. Those genes were heterologously expressed, and their properties were analyzed.

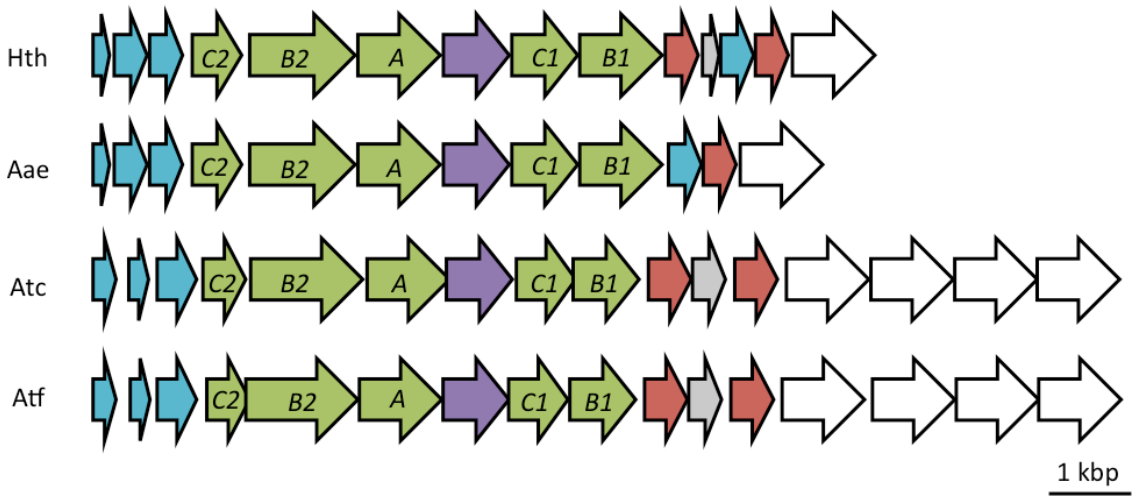

Fig. 1-10 Organization of *hdr* clusters in diverse bacteria. Predicted functions of genes are represented by each color: green, energy conservation; red, glycine cleavage system, H protein; blue, sulfur carrier; purple, conserved hypothetical protein; gray, hypothetical protein; white, other proteins. Hth, *Hydrogenobacter thermophilus* TK-6 (NC_017161, from HTH_1886 (for left) to HTH_1873 (for right)); Aae, *Aquifex aeolicus* VF5 (NC_000918); Atc, *Acidithiobacillus caldus* SM-1 (NC_015850); Atf, *Acidithiobacillus ferrooxidans* ATCC 23270 (NC_011761).

Table 1-3 General information of genes in the *hdr* cluster in *H. thermophilus*

Locus tag	Gene name	Transmembrane region[*1]	Motif	Homology or predicted function
HTH_1886		0		Sulfur carrier, cytoplasmic sulfur trafficking
HTH_1885	*dsrE*	1		Sulfur carrier, cytoplasmic sulfur trafficking
HTH_1884		0		Sulfur carrier, cytoplasmic sulfur trafficking
HTH_1883	*hdrC2*	0	2x [4Fe-4S] clusters	Energy production and conversion
HTH_1882	*hdrB2*	0	FeS cluster?	Energy production and conversion
HTH_1881	*hdrA*	0	Flavin, [4Fe-4S] cluster	Energy production and conversion
HTH_1880		1		Hypothetical protein
HTH_1879	*hdrC1*	0	2x [4Fe-4S] clusters	Energy production and conversion
HTH_1878	*hdrB1*	0	FeS cluster?[*2]	Energy production and conversion
HTH_1877	*gcvH3*	0		Glycine cleavage system, H protein
HTH_1876		0		Hypothetical protein
HTH_1875		0		Sulfur carrier, cytoplasmic sulfur trafficking
HTH_1874	*gcvH4*	0		Glycine cleavage system, H protein
HTH_1873		0		Radical SAM domain protein

[*1] Transmembrane regions were predicted by TMHMM (http://www.cbs.dtu.dk/services/TMHMM/).

[*2] The conserved sequence (CCG domain, probable FeS cluster binding site (9)) is observed.

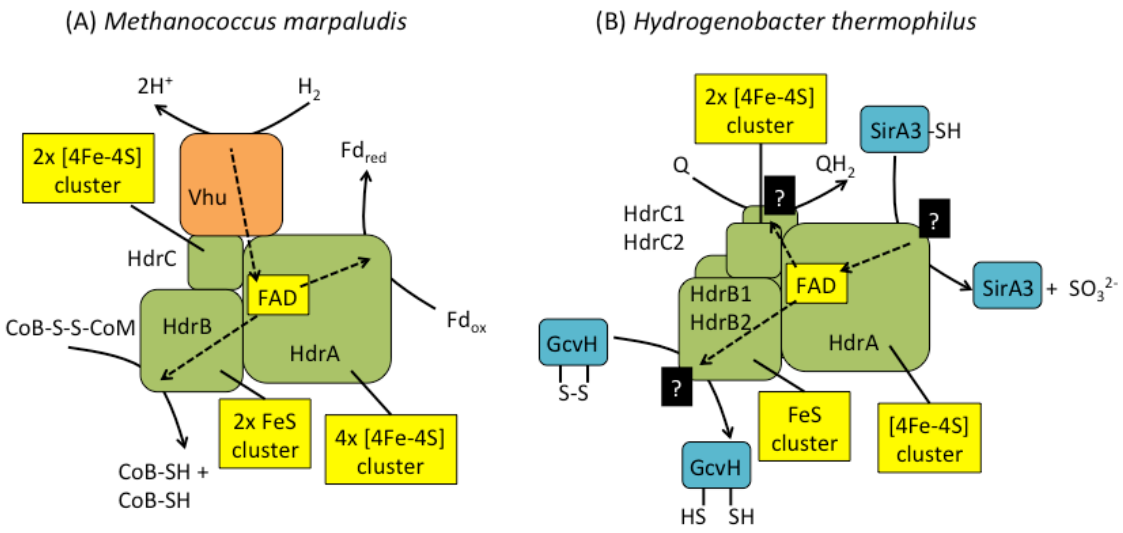

Fig. 1-11 Proposed model for Hdr reactions in *Methanococcus marpaludis* (A) and *H. thermophilus* (B). (A) Hdr complex in *M. marpaludis* oxidizes hydrogen, and reduces ferredoxin (Fd) and CoM-S-S-CoB coupling with Vhu hydrogenase by the electron bifurcating mechanism (8). (B) Predicted reaction model of Hdr complex in *H. thermophilus*. SirA is a candidate protein for a substrate of Hdr in *Aquifex aeolicus* (9). Predicted functions of proteins are represented for by each color: green, energy conservation; blue, sulfur carrier; orange, hydrogenase.

1-2-1 Materials and methods

Bacterial strain and growth condition. *H. thermophilus* TK-6 was cultivated under the hydrogen- or the thiosulfate-oxidizing condition at 70°C as described in chapter 1-1. *E. coli* JM109 and Rosetta^{TM}2(DE3) were utilized as the hosts of pET21c. *E. coli* strains were cultivated in Luria-Bertani (LB) medium. When required, 100 μg/mL ampicillin was supplied to the LB medium.

Construction of plasmids for heterologous expression. For heterologous protein expression, *gcvH3* (HTH_1877) gene and *gcvH4* (HTH_1874) gene were amplified by PCR by using the chromosomal DNA of *H. thermophilus* as a template without a stop codon to attach a 6x His-tag at the C-terminus of those genes. When *gcvH3* was cloned, non-sense mutation was introduced at Y115 to remove NdeI restriction site by using primers gcvH3-r-1 and gcvH3-f-2 in Table 1-4. The PCR fragment was digested with NdeI and XhoI, and then ligated into NdeI/XhoI-digested pET21c (Table 1-4). After confirmation of DNA sequence, those genes were expressed, and their product proteins were purified by the methods described below.

Table 1-4 List of primers used in chapter 1-2.

Primer	Sequence	Restriction site
gcvH3-f-1-NdeI	GTGCATATGGGACTAAGCGATGG	NdeI
gcvH3-r-1	CTCGCCATAAGGGTCGTAATTTATTATATC	
gcvH3-f-2	ACGACCCTTATGGCGAGGGC	
gcvH3-r-2-XhoI	CCACTCGAGTGTACACCTCATACAAAC	XhoI
gcvH4-f-NdeI	CTGCATATGGCTGTAGTTAACGGATGC	NdeI
gcvH4-r-XhoI	GATCTCGAGTCCGCACTTTATACCCTTC	XhoI

In the sequences, restriction sites are indicated by underline, and restriction enzymes are shown in the right columns.

Protein assay. The protein concentrations of samples were measured by using BCA protein assay kit (Pierce, Rockford, IL) with bovine serum albumin as the standard.

Protein preparation. Cell free extract (CFE), membrane fraction, and glycine cleavage proteins H3 (GcvH3) and H4 (GcvH4) of *H. thermophilus* were prepared as described below.

CFE of *H. thermophilus.* *H. thermophilus* wild type and mutant cells were cultivated under the hydrogen-oxidizing condition for 24 hours. After cultivation, 10 mM sodium thiosulfate was added, and the gas phase was changed to the gas mixture for the thiosulfate-oxidizing condition (N_2:O_2:CO_2 = 75:10:15 (v/v)). Cells were harvested at 5,000 x *g* for 10 min after 3 hours cultivation under the thiosulfate-oxidizing condition. The cells were disrupted by sonication with 50 mM Tris-HCl (pH 7.0). Cell debris was removed by ultracentrifugation (100,000 x *g* for 1 hour). The supernatant was used as CFE.

Membrane fraction of *H. thermophilus*. The pellet after the ultracentrifugation described in the preparation of the CFE of *H. thermophilus* was utilized. The pellet derived from approximately 1 g wet cells washed by 1 mL of 50 mM Tris-HCl (pH 7.0). The sample was centrifuged at 20,000 x *g* for 1 hour, and the supernatant was removed. The sample was resuspended in 1 mL of the same buffer containing 30 mg of *n*-dodecyl-β-D-maltoside (DDM) and incubated at 40°C for 1 hour. After the incubation, the sample was centrifuged at 20,000 x *g*, for 1 hour. The supernatant was utilized as the membrane fraction of *H. thermophilus*.

GcvH3 and GcvH4. *E. coli* Rosetta^{TM}2(DE3) harboring pET21c-*gcvH3* and pET21c-*gcvH4* were cultivated aerobically in LB medium containing 100 μg/mL ampicillin at 37°C. When the optical density (OD) at 600 nm of the culture became 0.6, 0.2 mM IPTG and 150 μM α-lipoic acid were added to the medium. After further cultivation for 6 hours, cells were harvested at 7,000 x *g* for 10 min. The cells were suspended in 50 mM Tris-HCl buffer (pH 7.0) and disrupted by sonication by using Ultrasonic disruptor at 100 W using a 50% duty for 15 min. The sonicated sample was heat-treated at 70°C for 10 min. The heat-treated sample was centrifuged at 7,000 x *g*

for 20 min to remove the denatured proteins and cell debris. The supernatant was applied onto Ni Sepharose 6 Fast Flow column (GE Healthcare) equilibrated with 50 mM Tris-HCl buffer (pH 7.0). Proteins were eluted with the same buffer containing 100 mM imidazole. Then, chromatography was performed aerobically with ÄKTApurifier system at room temperature. Mono Q 5/50 GL column (GE Healthcare) was used for the second purification step. The sample was applied onto the column equilibrated with the same buffer and eluted with a linear gradient from 0 to 1 M NaCl in the same buffer. The fractions containing GcvH3 and GcvH4 were used for the analyses.

Detecting protein-protein interaction. Swollen 500 μL of Ni sepharose 6 fast flow (GE healthcare) was washed with 50 mM Tris-HCl (pH 7.4) (buffer A). The gel was gently mixed overnight at 4°C with 10.5 mg of GcvH3 or GcvH4 in the buffer A. The gel was packed to an open column and equilibrated with the buffer A. Then, 5 mg protein of CFE or membrane fraction of *H. thermophilus* was applied to the column. Unbound proteins were eluted with 6 mL of the buffer A. Bound proteins were eluted with 6 mL of the buffer A containing 500 mM imidazole. Negative control experiment was performed by using the control column, which has no ligand protein. Protein bands were confirmed by SDS-PAGE.

1-2-2 Results

Heterologous expression and purification of GcvH3 and GcvH4.

GcvH3 and GcvH4, the two GcvH homologs encoded by the genes in the *hdr* cluster of *H. thermophilus*, were expressed in *E. coli* under the control of the T7 promoter in the pET21c vector. These proteins were purified by a combination of heat treatment, Ni-affinity chromatography, and anion exchange chromatography. Multiple bands appeared on SDS-PAGE in both purified fractions GcvH3 and GcvH4 (Fig. 1-12 (A) and 1-13 (A)). Typically, GcvH undergoes lipoylation after translation. It is thought that appearance of multiple bands in GcvH3 and GcvH4 might occur through an incomplete post-translational modification. Bands of GcvH3 and GcvH4 proteins appeared around 20 kDa and 15 kDa on SDS-PAGE, corresponding to the calculated molecular mass of monomeric GcvH3 and GcvH4 based on the sequence of those genes (18.1 kDa for GcvH3 and 15.5 kDa for GcvH4).

To determine the subunit compositions of GcvH3 and GcvH4, gel filtration was performed (Fig. 1-12 and 1-13). The molecular masses of GcvH3 and GcvH4 were estimated to be 27.8 kDa and 18.1 kDa, respectively, suggesting that these proteins exist as a monomer (Fig. 1-12 (B) and 1-13 (B)).

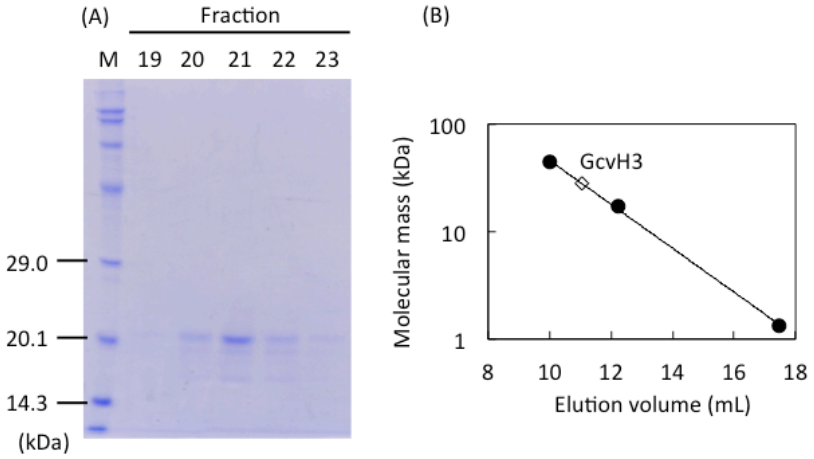

Fig. 1-12 Characterization of GcvH3 *of H. thermophilus*. (A) SDS-PAGE analysis of GcvH3 after the gel filtration on 18% acrylamide gel. A 15- μL of each fraction was applied. The band of GcvH3 was confirmed around 20 kDa. (B) Elution profiles of GcvH3 and molecular standards. Subunit composition of GcvH3 in the solution was determined by gel filtration using a Superdex^{TM} 75 10/300 GL (GE healthcare) column equilibrated with 50 mM Tris-HCl (pH 7.4). Gel filtration standard (Bio-Rad) was used as the standard. The profiles of the standards are as follows: ovalbumin, 44 kDa; myoglobin, 17 kDa; vitamin B_{12}, 1,350 Da. The molecular mass of GcvH3 was calculated to be 27.8 kDa.

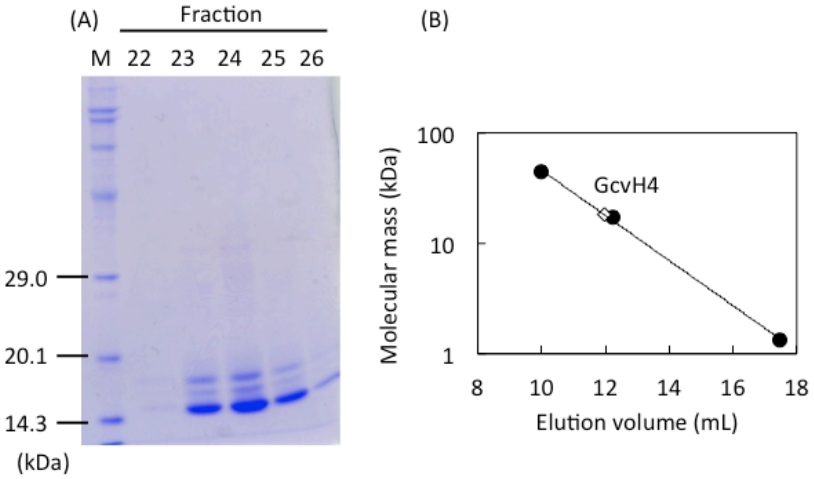

Fig. 1-13 Characterization of GcvH4 of *H. thermophilus*. (A) SDS-PAGE analysis of GcvH4 after the gel filtration on 18% acrylamide gel. A 15- μL of each fraction was applied. The band of GcvH4 was confirmed around 15 kDa. (B) Elution profiles of GcvH4 and molecular standards. Subunit composition of GcvH4 in the solution was determined by gel filtration using a Superdex^{TM} 75 10/300 GL (GE healthcare) column equilibrated with 50 mM Tris-HCl (pH 7.4). Gel filtration standard (Bio-Rad) was used as the standard. The profiles of the standards are as follows: ovalbumin, 44 kDa; myoglobin, 17 kDa; vitamin B_{12}, 1,350 Da. The molecular mass of GcvH4 was calculated to be 18.1 kDa.

Detection of GcvH-interacting protein.

To search for proteins that interact with GcvH3 and GcvH4, chromatography using those proteins as a bait was performed (Fig. 1-14 and 1-15). Purified GcvH3 and GcvH4 were absorbed on a Ni-affinity column, and cell free extract or membrane fraction of *H. thermophilus* was applied. Then, bound proteins were eluted by the buffer containing 500 mM imidazole, and the presence of the proteins was checked by SDS-PAGE. As a result, no significant protein from the prey fraction was detected in the bound fractions (Fig. 1-14 and 1-15). It was considerable that the interaction between GcvH proteins and prey proteins was too weak to keep prey proteins in the Ni-affinity column.

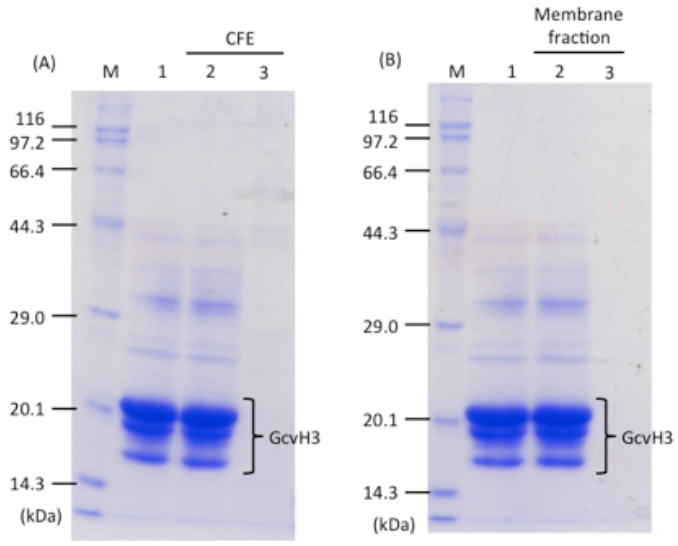

Fig. 1-14 Detection of GcvH3 associated protein by SDS-PAGE. (A) CFE and (B) membrane fraction of *H. thermophilus* were utilized as the prey proteins. Purified GcvH3 (lanes 1), the bound fractions from the Ni Sepharose 6 Fast Flow column on which GcvH3 was absorbed (lanes 2), and the bound fractions from the column without GcvH3 (lanes 3, negative control).

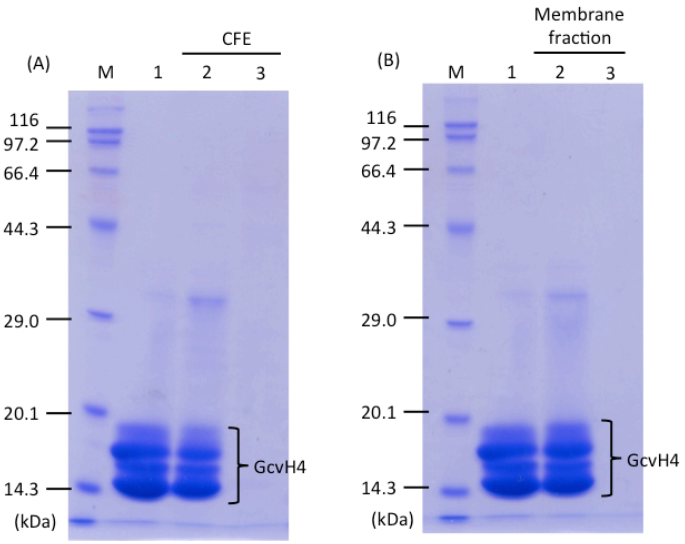

Fig. 1-15 Detection of GcvH4 associated protein by SDS-PAGE. (A) CFE and (B) membrane fraction of *H. thermophilus* were utilized as the prey proteins. Purified GcvH4 (lanes 1), the bound fractions from the Ni Sepharose 6 Fast Flow column on which GcvH4 was absorbed (lanes 2), and the bound fractions from the column without GcvH4 (lanes 3, negative control).

1-2-3 Discussion

The properties of GcvH3 and GcvH4 present in the *hdr* cluster of *H. thermophilus* were investigated in this section. Two proteins were purified to characterize GcvH-related proteins. The fractionations of CFE and membrane fraction were performed using a GcvH-affinity column, but this approach did not work well probably due to the weak protein-protein interaction (Fig. 1-14 and 1-15).

A redox potential of S^{2-}/SO_3^{2-} is predicted to be about -170 mV (9). Meanwhile, those of α-lipoic acid, which is covalently linked to a lysyl residue of the GcvH, and a quinone (menaquinone) are about -320 mV and -74 mV, respectively (9, 10). Therefore, it is expected that Hdr performs a down-hill reaction (reduction of quinone) and an up-hill reaction (reduction of GcvH) simultaneously in electron bifurcation if GcvH serves as an electron acceptor for Hdr as I hypothesized.

Reduced GcvH can be reoxidized in two pathways. (i) The proteins encoded in *hdr* cluster may have functional relationship with those in *hyn* cluster because expression levels of the latter were repressed in Δ*hdrA* as shown in chapter 1-1. Since Isp2 present in the *hyn* cluster has homology with heterodisulfide reductase (11), reduced GcvH may be oxidized by Isp2 as an electron carrier. (ii) *H. thermophilus* has two putative genes encoding L-proteins of glycine cleavage system (HTH_0448, 1209). In the glycine cleavage system in general microbes, L-proteins reduce NAD^+ (E_0' = -320 mV) by oxidizing –SH groups of the α-lipoic acid in GcvH. Therefore, the GcvH homologs in *H. thermophilus* may play a role in the reduction of NAD^+ in the thiosulfate-oxidizing metabolism. In any case, determining the reaction partner of Hdr is important for a deeper understanding of *H. thermophilus* physiology.

Chapter 2 Sulfite-oxidizing enzyme

2-0 Introduction

Sulfite is one of the major intermediate metabolites produced in the oxidation process of sulfur. Sulfite has high reactivity due to nucleophilicity and strong reducing power (E_0' = -515 mV for the SO_4^{2-}/SO_3^{2-} couple) and easily reacts with DNA and protein (1, 2). Both prokaryotic and eukaryotic organisms have developed efficient oxidation mechanisms to detoxify sulfite.

The most well studied periplasmic sulfite:cytochrome *c* oxidoreductase in prokaryotes is SorAB in *Starkeya novella* (Fig. 2-1, Table 2-1) (3). This protein consists of SorA containing a molybdopyranopterin as a co-factor subunit and monohaem cytochrome *c* (SorB). Homologs of these two genes are present in the *H. thermophilus* genome (HTH_0806 and HTH_0807).

While this enzyme is usually localized in the periplasm, another sulfite-oxidizing pathway employs the reverse reaction of assimilatory sulfate reduction in the cytoplasm (Fig. 2-1). In this pathway, adenosine-5'-phosphosulfate (APS) is formed from sulfite and AMP by APS reductase, and the AMP moiety of APS is subsequently transferred to pyrophosphate by ATP sulfurylase, generating sulfate and ATP. *A. aeolicus,* a closely related species of *H. thermophilus*, is able to oxidize sulfite and obtains ATP through this pathway (4). Although *H. thermophilus* also has a gene set of assimilatory sulfate reduction pathway (HTH_0442-0449), the expression levels of these genes are repressed under the thiosulfate-oxidizing condition (5). Thus, it was suspected that sulfite oxidation operates not thorough the assimilatory sulfate reduction pathway but thorough another unrevealed pathway in *H. thermophilus*.

Recently, it was reported that cytoplasmic enzymes named SoeABC (sulfite-oxidizing enzyme) serve as the main player of sulfite oxidation in a purple sulfur bacterium, *Allochromatium vinosum* (6). SoeABC is an enzyme belonging to the molybdenum-containing protein family and consists of a catalytic subunit containing molybdopterin as the co-factor (SoeA), an iron-sulfur cluster subunit (SoeB), and a transmembrane subunit (SoeC). In the *H. thermophilus* genome, there is a gene set of the molybdenum-containing family proteins annotated as a sulfur reductase (SreABC, HTH_1746, 1741, and 1740), which shares high sequence similarity with *A.vinosum*

SoeABC.

Molybdenum-containing protein family is known to have diverse functions. I collected the sequences of catalytic subunit of this family and constructed a phylogenetic tree with SreA of *H. thermophilus* (Fig. 2-2). As a result, SreA of *H. thermophilus* was phylogenetically closer to SoeA of *A. vinosum* rather than to other enzymes, such as sulfur reductase. Therefore, in this chapter, I focused on SreABC to elucidate the sulfite oxidation mechanism in *H. thermophilus*.

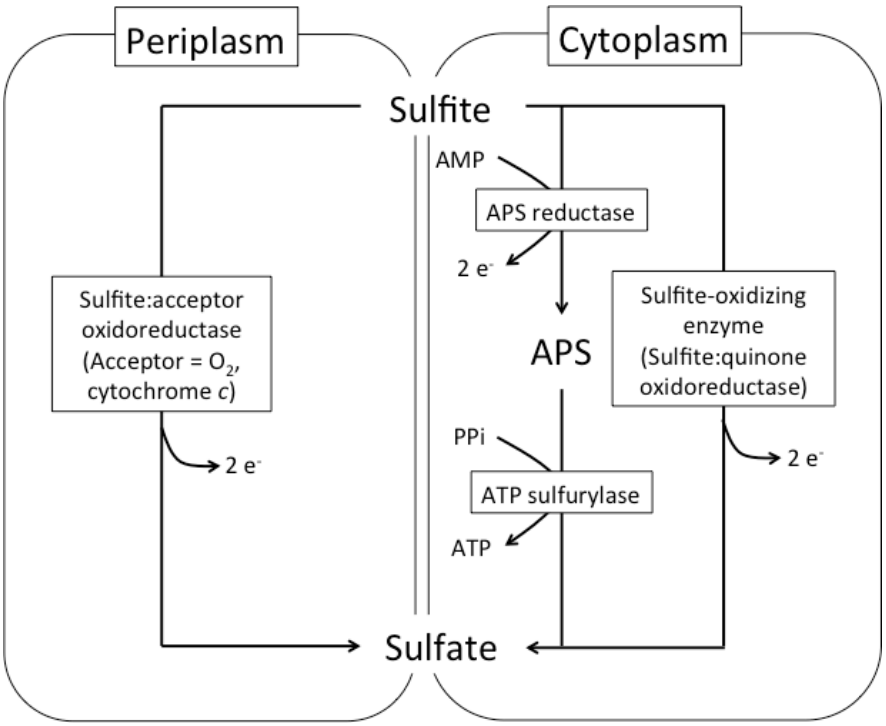

Fig. 2-1 The pathways of sulfite oxidation. Direct and indirect sulfite oxidation pathways. The former pathways are catalyzed by a single enzyme (sulfite:acceptor oxidoreductase or sulfite:quinone oxidoreductase), while the latter pathway is catalyzed by two sequential enzymes (APS reductase and ATP sulfurylase). *H. thermophilus* has sulfite:acceptor oxidoreductase (HTH_0806 and 0807), but not the indirect sulfite oxidation pathway. Genes encoding a homolog of sulfite-oxidizing enzyme were found, recently (HTH_1746, 1741, and 1740).

Table 2-1 List of enzymes for sulfite oxidation.

Enzyme	Organism	Electron acceptor	Localization	Homologs in *H. thermophilus*
SorAB	*S. novella*	Cytochrome *c*	Periplasm	HTH_0806 and 0807 (SorAB)
SoeABC	*A. vinosum*	Quinone	Cytoplasm	HTH_1746, 1741, and 1740 (SreABC)

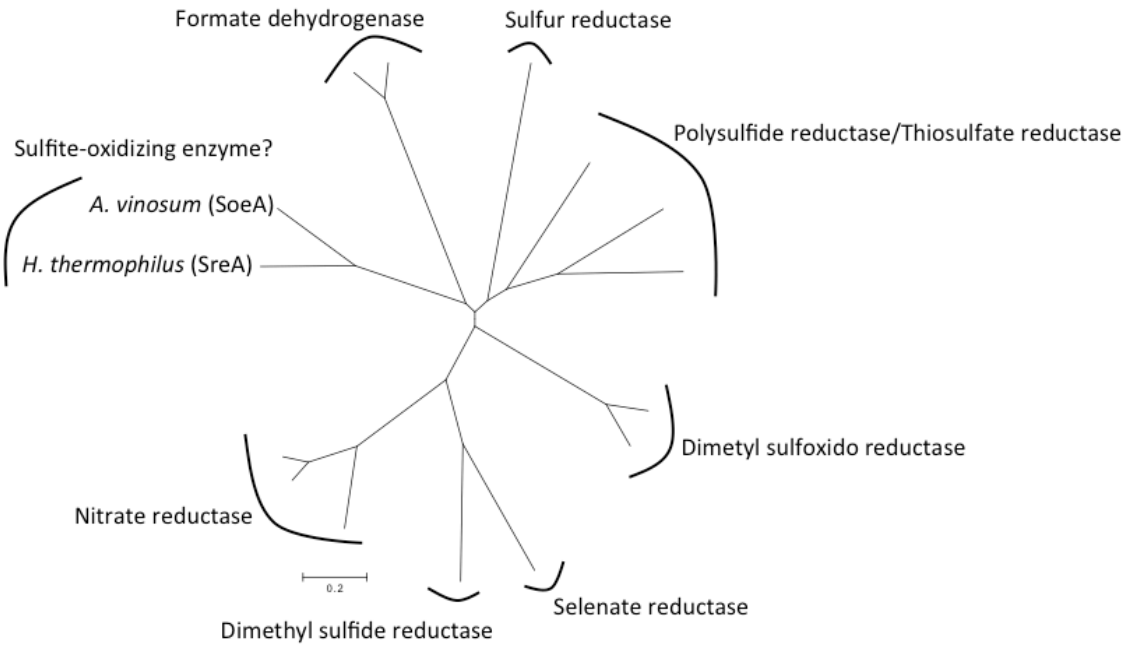

Fig. 2-2 Phylogenetic tree of catalytic subunit of molybdenum containing enzyme family proteins. The protein sequences of molybdenum containing enzyme family which is reviewed in Uniprot was collected. The sequence of SreA of *H. thermophilus* together with 14 data was analyzed, and a phylogenetic tree was drawn by the neighbor-joining method. The genes and its Uniprot ID used for construction of phylogenetic tree were as follows; *Hydrogenobacter thermophilus* (*sreA*, D3DK38), *Allochromatium vinosum* (*soeA*, D3RNN8), *Salmonella typhimurium* (*phsA*, Q72LA4), *Thermus thermophilus* (*psrA*, Q72LA4), *Wolinella succinogenes* (*psrA*, P31075), *Acidiunus ambivarens* (*sreA*, Q8NKK1), *Escherichia coli* (*narG*, *narZ*, *dmsA*, *fdnG* and *fdoG*, P09152, P19319, P18775, P24183 and P32176), *Haemophilus influenzae* (*dmsA*, P45004), *Thauera selenatis* (*serA*, Q9S1H0), *Rhodovulum sulfidophilum* (*ddhA*, Q8GPG4) and *Bacillus subtilis* (*narG*, P42175).

2-1 Materials and methods

Bacterial strain and growth condition. *H. thermophilus* TK-6 was cultivated at 70°C in a sulfate-limited inorganic medium in a 100-mL vial. Hydrogen or sodium thiosulfate was utilized as an energy source. For the thiosulfate-oxidizing growth, 10 mM sodium thiosulfate was supplied to the medium. The gas phase in the vial was replaced with gas mixtures of H_2:O_2:CO_2 (75:10:15) and N_2:O_2:CO_2 (75:10:15) for the hydrogen-oxidizing condition and the thiosulfate-oxidizing condition, respectively. For the anaerobic growth, 47 mM sodium nitrate or 100 mM elemental sulfur were supplemented to the medium, and the gas phase in the vial was replaced with gas mixtures of H_2:N_2:CO_2 (75:10:15) and N_2:CO_2 (85:15) for the hydrogen-oxidizing condition and the thiosulfate-oxidizing condition, respectively.

Construction of a Δ*sreA* mutant. The method for gene disruption of *H. thermophilus* was described in chapter 1-1. A plasmid for gene disruption was constructed and used for mutant construction according to the homologous recombination method reported in a previous study (Fig. 2-3 and Table 2-2).

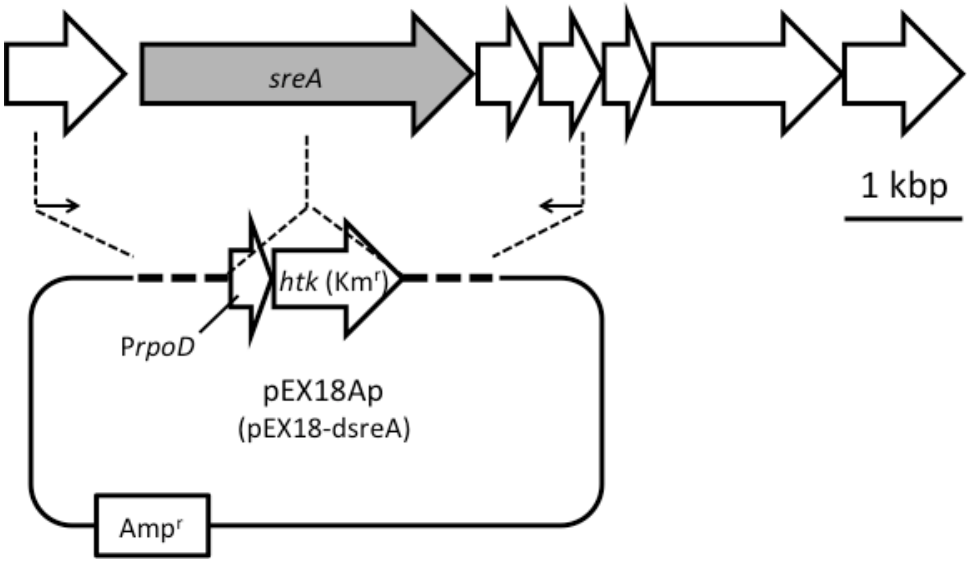

Fig. 2-3 Scheme for construction of the plasmid. Gray arrow indicates targeted gene for disruption. The dashed lines in the plasmid regions shares identical sequence with the chromosomal DNA of *H. thermophilus*. The small arrows indicate the binding site of the primers used for PCR. *htk*, highly thermostable kanamycin resistance gene fused with promoter region of *H. thermophilus rpoD* gene (P*rpoD*); Km, kanamycin; Amp, ampicillin.

Table 2-2 List of primers used in chapter 2.

Primer	Sequence	Restriction site
SreA_dis_F	CATGCATGCGTCCACTATC	SphI
SreA_dis_R	AAAGAGCTCTCTTAAGGTGCTG	SacI

In the sequence, restriction sites are indicated by underline, and restriction enzymes are shown in the right column.

Detection of sulfur compounds. Thiosulfate and sulfate were determined by colorimetric or turbidometric methods as described in chapter 1-1. Sulfite and sulfide were also determined by colorimetric methods.

Sulfite. Sulfite was determined via fuchsin method (7). A 690-µL sample was incubated with 200 µL of 2% zinc acetate and 100 µL 0.04% fuchsin (in 10%, v/v, H_2SO_4) for 10 min at room tempearature. After incubation, 10 µL of 35% (v/v) formaldehyde was added, and the mixture was incubated for another 10 min at room temperature. The absorbance of a Schiff base at 570 nm was measured.

Sulfide. A 700- µL sample was incubated with 200 µL of 2% zinc acetate, 100 µL of 0.2% DPPDS reagent (Dimethyl-*para*-phenylenediamine sulfate (DPPDS) in 14%, v/v, H_2SO_4) and $Fe(NO_3)_3$ reagent (15 g of $Fe(NO_3)_3 \bullet 9H_2O$ and 17 mL of 65% (v/v) HNO_3 made up to 50 mL with deionized water) for 20 min at room temperature. The absorbance of a methylene blue at 670 nm was measured (8).

Protein assay. The protein concentrations of samples were measured by using BCA protein assay kit (Pierce, Rockford, IL) with bovine serum albumin as the standard.

Protein preparation. Membrane fraction and cell free extract (CFE) of wild type and Δ*sreA* of *H. thermophilus* was prepared as described in chapter 1-2.

Cytochrome *c*. Cytochrome c_{552} was purified as described below. *H. thermophilus* CFE was applied to a TOYOPEARL® CM-650S column (Tosoh) equilibrated with 50 mM Tris-HCl (pH 7.0). The cytochrome *c* fraction was eluted by 10 mL of the same buffer containing 100 mM NaCl. After the concentration of the sample by VIVASPIN 20 (3,000 MWCO PES, Sartorius), the sample was applied to a Superdex 75 10/300 GL column (GE healthcare) equilibrated with the same buffer. ÄKTA purifier system was used for the gel filtration step.

Activity measurement sulfite-oxidizing enzyme. I tried to measure the activity of sulfite-oxidizing enzyme using three methods: activity staining, colorimetric assay and oxygen consumption assay.

Activity staining assay (9). Activity staining was performed using a gel after blue native (BN)-PAGE. SuperSep^{TM}Ace, 5-12%, 13well (Wako) was used for BN-PAGE. The gel was immersed in a solution containing 1 mM sodium sulfite, 1 mM potassium ferricyanide, 0.1 mM EDTA and buffer solution for 1 hour at room temperature. Three kinds of buffers (100 mM Bis-Tris-HCl(pH 7.0), Tris-HCl (pH 8.0) and 100 mM Bicine-NaOH (pH 9.0)) were used. The gel was briefly washed in deionized water and immersed in 10 mM ferric chloride. A blue band of Prussian blue was checked. The gel was also subjected to Coomasie Brilliant Blue (CBB) staining.

Colorimetric assay. Sulfite-oxidizing enzyme activity was assayed by monitoring the reduction of oxidized methyl viologen. Enzyme assay was performed in 100 mM Tris-HCl buffer (pH 8.0) containing 0.5 mM sodium dithionite, 0.05% of *n*-dodecyl-β-D-maltoside (DDM), 5 mM methyl viologen, 5 mM sodium sulfite and 1 mg protein of membrane fraction. The cuvette was sealed with a rubber septum and an aluminum cap, and its head space was replaced with nitrogen. The reaction was started by the addition of sodium sulfite at 70°C, and the absorbance of the reduced methyl viologen at 604 nm was monitored.

Oxygen consumption assay. The scheme of oxygen consumption assay is shown in Figure 2-4. At first, an electron acceptor (quinone) is reduced by the addition of an electron donor (sulfite). Subsequently, oxygen is consumed when the electron acceptor is oxidized by terminal oxidases. The consumption of oxygen during the reaction was measured using an oxygen electrode. APOLLO 4000 Free Radical Analyzer (World Precision Instruments) was used to monitor the reaction. The reaction was performed at 37°C in 50 mM Tris-HCl (pH 7.0) buffer containing 2.5 mg protein of membrane fraction and 5 mM sodium sulfite, and the reaction was started by addition of sodium sulfite.

Activity measurement of sulfite:cytochrome *c* oxidoreductase (SOR). SOR activity was assayed by monitoring the reduction of cytochrome *c* (cyt. *c*) purified from *H. thermophilus*. Enzyme assay was performed in 20 mM Tris-HCl buffer (pH 8.0) containing 0.1 mg cyt. *c*, 2.5 mM sodium sulfite and 0.5 mg protein of CFE in a total volume of 500 µL. The reaction was started by addition of sodium sulfite at 70°C, and the absorbance of the reduced cyt. *c* at 552 nm was monitored. The concentration of the reduced cyt. *c* was calculated using a molar extinction coefficient of 19 mM^{-1}.

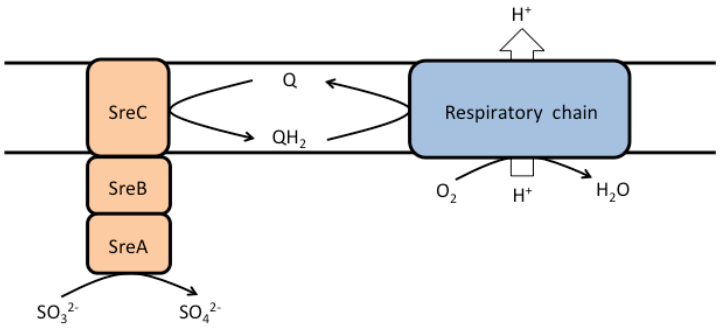

Fig. 2-4 The scheme of the oxygen consumption assay. Consumption of oxygen by oxidation of quinol in the respiratory chain is measured. If the sulfite-oxidizing enzyme reacts with sulfite in a quinone-depending manner, a decrease of dissolved oxygen would be observed.

2-2 Results

本項の内容は、学術雑誌論文として出版する計画があるため公表できない。5 年以内に出版予定である。

2-3 Discussion

In this chapter, I focused on the sulfite-oxidizing enzyme in *H. thermophilus*. In growth test, Δ*sreA* accumulated sulfite in the culture medium compared to wild type. This result suggested that SreA in *H. thermophilus* functions as a sulfite-oxidizing enzyme *in vivo*.

The sulfite-oxidizing enzyme in *A. vinosum* is reported to function in cytoplasm (6). In the *H. thermophilus* genome, HTH_0445 located in a gene cluster for assimilatory sulfate reduction has a homology with a sulfite exporter. It is considerable that this gene product transported sulfite to the outside of the cell. On the other hand, the gene cluster of this pathway was down-regulated in wild type when it was cultured under the thiosulfate-oxidizing condition. The presence of intracellular sulfite may regulate the expression of these genes.

Although the growth profiles of Δ*sreA* suggested that SreA plays a role for sulfite oxidation, its activity could not be measured *in vitro*. Molybdopterin, a co-factor of sulfite-oxidizing enzyme, is generally known to be very sensitive to oxygen. The loss of co-factor may be the reason why the activity measurements were not succesful.

Significant sulfite oxidation was observed after 40 hours cultivation in Δ*sreA*. *H. thermophilus* has not only sulfite-oxidizing enzyme but also sulfite:cytochrome *c* oxidoreductase (SOR). It was considerable that SOR oxidized sulfite at this point. The SOR activity in *H. thermophilus* CFE was measured by the colorimetric method, in which reduction of cytochrome *c* was monitored (Fig. 2-11). As a result, SOR activity was confirmed in both wild type and Δ*sreA*, and also, Δ*sreA* seemed to have higher activity than wild type. The enhanced SOR activity in Δ*sreA* may have been caused by the higher accumulation of sulfite in the culture medium (Fig. 2-6 (C)). Since SOR genes (*sorA* and *sorB*) have signal peptides, SOR probably functions in periplasm. *H. thermophilus* may use two enzymes for sulfite oxidation depending on the localization.

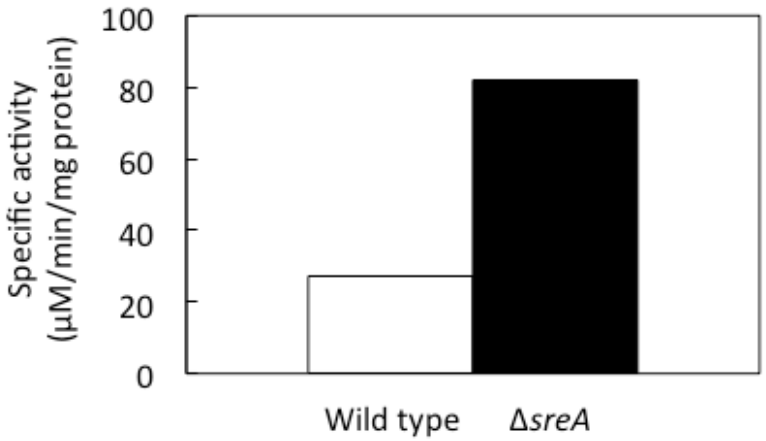

Fig. 2-11 Activity for oxidation of sulfite by sulfite:cytochrome *c* oxidoreductase in *H. thermophilus* wild type and Δ*sreA*. Cell free extracts of wild type (open bar) and Δ*sreA* (closed bar) were used as the enzyme source.

Chapter 3 Sulfur globule

3-0 Introduction

Microorganisms have the ability to interact with solid materials and utilize them as an electron acceptor or electron donor. For example, our laboratory revealed that some obligate anaerobic bacteria, *Sporomusa ovata*, *Clostridium autoethanogenum*, and *Clostridium carboxidivorans*, could grow using solid iron as the sole energy source (1). Microorganisms also produce insoluble materials as metabolites; sulfur globule produced as an intermediate of sulfur metabolism is one example. Some sulfur-oxidizing bacteria accumulate sulfur globule inside or outside of the cells. *Acidithiobacillus caldus* is a β-proteobacteria that accumulates extracellular sulfur globules (2). It is revealed that the gene expression of outer membrane proteins and secretion proteins was significantly changed in *A. caldus* when sulfur globule is used as an energy source (2). Intracellular sulfur globules produced by *Allochromatium vinosum* have been studied in terms of their synthesis and degradation (3). Sulfur globules accumulated in the periplasm of *A. vinosum* are coated with proteins called sulfur globule protein (Sgp) (4). Sgp is encoded by three genes, *sgpA*, *sgpB*, and *sgpC*. SgpA and SgpB are the functionally homologous to each other. Mutation analysis suggested that SgpC is involved in the formation of sulfur globule (3). *Chlorobium tepidum*, a model organism of green sulfur bacteria, also forms extracellular sulfur globule (5), and two kinds of proteins with unknown functions (CT1320.1 and CT1305) were isolated from its sulfur globule (6). These *C. tepidum* proteins share no significant homology with Sgp of *A.vinosum*.

In *H. thermophilus*, sulfur globules are observed outside the cells when the cells are cultivated under the thiosulfate-oxidizing condition. *H. thermophilus* metabolizes thiosulfate to sulfate and insoluble sulfur species via the sox system in the periplasmic space. The insoluble sulfur species produced are transported to cytoplasm and then oxidized by the Hdr enzyme as discussed in the chapter 1. However, some insoluble sulfur species are released to the outside of the cells by an unknown cellular mechanism and observed as sulfur globules.

Very little is known about the sulfur globule of *H. thermophilus*. Therefore, I focused on the sulfur globules produced by *H. thermophilus* to clarify its properties.

3-1 Material and method

Bacterial strain and growth condition. *H. thermophilus* TK-6 was cultivated at 70°C in a sulfate-limited inorganic medium in a 100-mL vial. Hydrogen or sodium thiosulfate was utilized as an energy source. For the thiosulfate-oxidizing growth, 10 mM sodium thiosulfate was supplied to the medium. The gas phase in the vial was replaced with gas mixtures of H_2:O_2:CO_2 (75:10:15) and N_2:O_2:CO_2 (75:10:15) for the hydrogen-oxidizing condition and the thiosulfate-oxidizing condition, respectively.

Purification of sulfur globule. *H. thermophilus* wild type and mutant cells were cultivated under the hydrogen-oxidizing condition for 24 hours. After cultivation, 10 mM sodium thiosulfate was added, and the gas phase was changed to the gas mixture for the thiosulfate-oxidizing condition (N_2:O_2:CO_2 = 75:10:15 (v/v)). Cells were harvested at 5,000 x *g* for 10 min after 3 hours cultivation under the thiosulfate-oxidizing condition.

Sulfur globule was purified from the cultures by sucrose density gradient centrifugation (6). The mixture of sulfur globules and cells harvested from 1 L of culture medium were suspended in the small amount of sulfate-limited medium. The suspension was layered over 40 mL of 2.5 M sucrose solution in a 50-mL tube. The sulfur globule was pelleted via the sucrose by centrifugation at 4,000 x *g*, for 10 min, at room temperature. The collected pellet was centrifuged via sucrose two more times. The collected sulfur globule was resuspended in 1 mL of deionized water and centrifuged at 17,500 x *g*, for 5 min to remove sucrose completely. This step was repeated twice. Sulfur globule was resuspended in 1 mL of deionized water and incubated for 30 min without centrifugation. The supernatant was carefully removed, and the precipitation was used as the sulfur globule fraction.

Measurement of the particle size of sulfur globule. The particle size of sulfur globule was measured using Zetasizer APS (Malvern) by the dynamic light scattering method. The calculation was based on the assumptions that the solvent is water and that the particle shape is sphere. The sample was diluted 2,000 times with distilled water and measured at 20°C. The particle size was calculated from triplicated

measurements.

Detection of sulfur globule-associated proteins. Equal amount of 10% sodium dodecyl sulfate (SDS) was mixed with the sulfur globule fraction. The mixture was centrifuged at 10,000 x *g*, for 10 min. The supernatant was applied to SDS-PAGE. The protein in the sulfur globule fraction was identified by N-terminal amino acid sequencing. Proteins were separated by SDS-PAGE and transferred onto the PVDF membrane by using a semidry system. The N-terminal amino acid sequence was determined using Procise 491 cLC protein sequencer (Applied biosystems).

3-2 Results and discussion

Purification of sulfur globule.

Sulfur globule was purified from *H. thermophilus* cultured under the thiosulfate-oxidizing condition and was observed with a microscope (Fig. 3-1). No bacterial contamination was observed in sulfur globules (Fig. 3-1 (B)). The shape of sulfur globule was sphere, and some globules were aggregated. I tried to measure the size of the sulfur globule using a zetasizer. As a result, three particle sizes (about 70 nm, about 300 nm and about 2 μm) were obtained (Table 3-1). Values around 2 μm were confirmed in any trial. These large particle sizes may be derived from sulfur globules aggregated during sample preparation or measurements. On the other hand, the other two small values were not always available. It was thought that the influence of gravity caused by aggregation of sulfur globules made the measurement unstable.

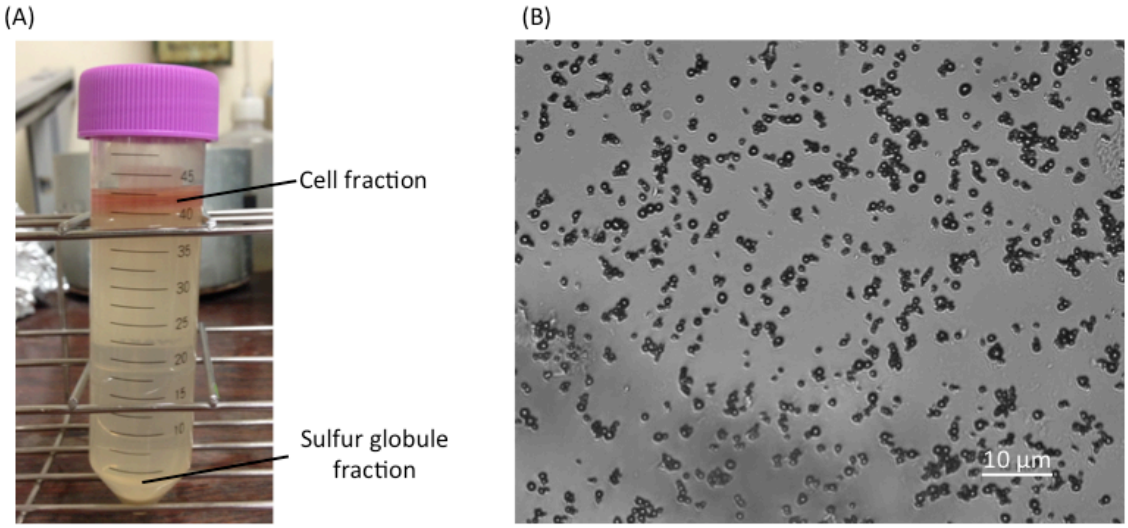

Fig. 3-1 Purification of sulfur globules. (A) Separation by the sucrose density gradient centrifugation method. The upper layer is the cell fraction, and the lower white layer is the sulfur globule fraction. (B) Microscopic image of sulfur globule. Sulfur globule fraction was observed at 400x magnification using Axioplan 2 imaging microscope (Carl Zeiss).

Table 3-1 The size of sulfur globules measured by a zetasizer.

Well	Trial	Size 1 (nm)	Size 2 (nm)	Size 3 (nm)
A4	1		930.6	2509
	2	87.4		1819
	3			1534
A5	1	36.9	305.2	2780
	2	100.9		2528
	3	53.5	201.3	2720
A6	1	106.8		2253
	2		138.7	1993
	3		176.7	1421
	Average	77.1±30.5	350.5±330.1	2173±506

Extraction and identification of sulfur globule-associated protein.

Proteins were extracted from sulfur globules of *H. thermophilus*, and SDS-PAGE was performed to check whether the sulfur globules contained proteins. The result of SDS-PAGE clearly showed that significant amount of proteins was contained in the globules and that the protein(s) that appears as a single band was dominant in the extract (Fig. 3-2). The protein band was identified by N-terminal amino acid sequencing. The amino acid sequence of the protein was determined to be AERQAP. By comparing this sequence with *H. thermophilus* genome, it was revealed that the sequence corresponded to a tetratricopeptide repeat (TPR) protein (HTH_0586). General information of HTH_0586 deduced from its primary structure is shown in Table 3-2. This gene product was homologous neither to the Sgp of *A. vinosum* nor to the sulfur-associated proteins of *C. tepidum*. Therefore, this gene product is suggested to be a novel protein that forms a complex with sulfur globule.

TPR protein is a protein originally identified in yeast (7, 8), and is widely conserved in many organisms. A single TPR motif consists of 34 residues and forms antiparallel α-helices. This motif can be found in various proteins, present in tandem arrays of 3-16 repeating motifs (9). HTH_0586 preserves seven TPR motifs (Fig. 3-3). The general function of TPR motif is a mediation of protein-protein interaction, and thus TPR motif is involved in various cell processes as a scaffold (10). In addition to the TPR motif, HTH_0586 has a signal sequence and typical lipobox (Fig. 3-3), suggesting that this protein is a periplasmic lipoprotein interacting with the membrane. PilF in *Pseudomonas aeruginosa*, an example of lipoproteins with TPR motif, is an essential component of type IV pilus (11). Type IV pilus has various functions, such as motility on solid surface, cell adhesion and protein uptake (12). It is considerable that a cellular component similar to type IV pilus contributes to the release or uptake (or both) of sulfur globules in *H. thermophilus*. However, no homology was found between overall sequences of HTH_0586 and PilF. The interaction between HTH_0586 and sulfur globules or pilus proteins also has yet to be clarified.

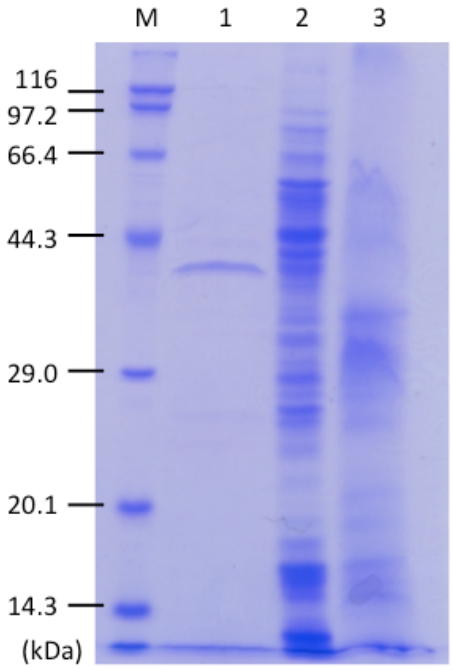

Fig. 3-2 Detection of the proteins solubilized from in the sulfur globule. Extract from sulfur globule (lane 1), cytoplasmic fraction (lane 2) and membrane fraction (lane 3) of *H. thermophilus* were applied to polyacrylamide gel (18%). Proteins were detected by CBB staining

Table 3-2 General information about HTH_0586.

Locus tag	Description	Expected molecular mass (kDa)	Localization*
HTH_0586	Tetratricopeptide repeat protein	34.7	Periplasm

*Localization of the protein was predicted by psortb (http://www.psort.org/psortb/).

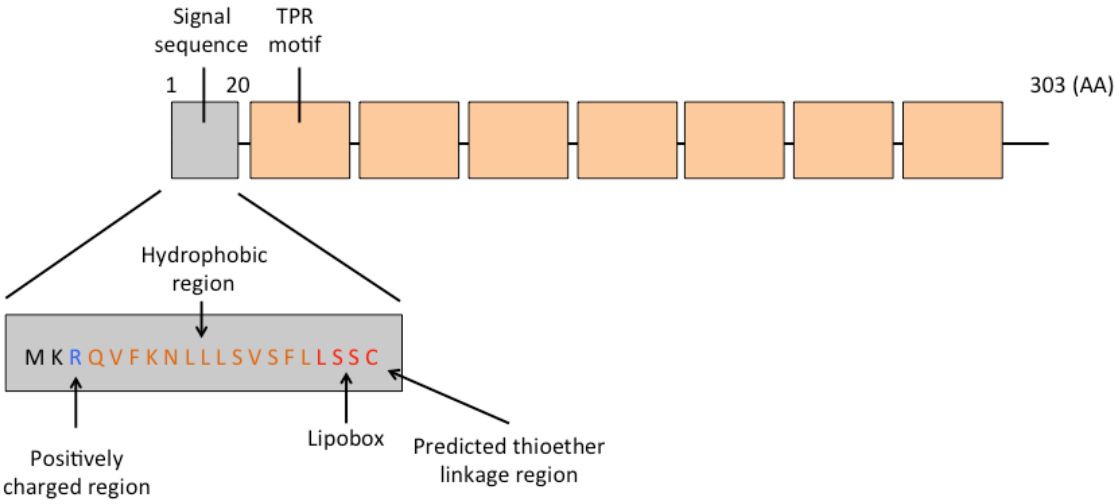

Fig. 3-3 The primary structure of HTH_0586 and the sequence of its peptide. Positively charged region, hydrophobic region, and typical lipobox suggest that HTH_0586 is a lipoprotein.

Conclusions and prospects

The purpose of this study is to clarify how *H. thermophilus* TK-6 utilizes thiosulfate as an energy source. The advantages of studying thiosulfate metabolism in this bacterium are given below: (i) this bacterium belongs to the oldest branch in the phylogenetic tree, so that features of ancient organisms may be found; (ii) this bacterium is chemolithoautotroph whose energy metabolisms are simple; (iii) omics information is available, and genetic manipulation techniques are established. In this research, I described the whole thiosulfate metabolism of *H. thermophilus*. What I found and the importance of this study is summarized as follows.

In chapter 1, physiology of *hdr* in *H. thermophilus* was characterized. Phenotype of Δ*hdrA* suggested that HdrA plays a role in energy acquisition and sulfur oxidation. Also, in microarray analysis, the gene set of *hyn* cluster was mentioned as a candidate gene related to *hdr*. The proteins in *hyn* cluster (HynL, HynS, Isp1 and Isp2) form a complex on the membrane and function as hydrogenase. Since Isp2 has heterodisulfide reductase activity, it was speculated that Hdr complex and Hyn complex may utilize GcvH as a common substrate, although I could not screen proteins interacting with GcvH3 and GcvH4.

H. thermophilus should oxidize intracellular sulfite in the process of thiosulfate oxidation because Hdr localizes in cytoplasm. Therefore, in chapter 2, cytoplasmic sulfite-oxidizing enzyme in *H. thermophilus* was investigated. Phylogenetic analysis and phenotype of Δ*sreA* suggested that SreABC functions as a sulfite-oxidizing enzyme *in vivo*. Several methods were used to measure the activity of this enzyme, but no activity was observed in any method. In addition to SreABC, *H. thermophilus* has another enzyme for sulfite oxidation, which is named SorAB (sulfite:cytochrome *c* oxidoreductase, HTH_0806 and 0807). This enzyme probably localizes in periplasm. From these results, it was suggested that sulfite produced in cytoplasm is oxidized by SreABC, and sulfite present outside the cell is removed by SorAB, respectively.

In chapter 3, sulfur globules, produced by *H. thermophilus* were investigated. Although it was difficult to determine accurate particle size due to aggregation, the size of sulfur globules was about several hundred nm. HTH_0586, which is a unique protein in sulfur globules, was identified. This was a novel protein because there was

no homology with known sulfur globule proteins.

The significance of this study is described below.

The first is that physiological and experimental evidences of thiosulfate-oxidizing enzymes of *H. thermophilus* have been obtained. In chapter 1, I showed the physiological function of *hdrA* as the sulfur-oxidizing enzyme for the first time using Δ*hdrA* strain. Also, in chapter 2, the function of *sreA in vivo* was clarified from analysis of Δ*sreA*.

The second is to show the fate of sulfur compounds in this bacterium. Gene functions involved in thiosulfate oxidation could be inferred by comparison of profiles of sulfur compounds over time between wild type and mutants. Moreover, by calculating sulfur atoms in the culture, it was suggested that there is unknown sulfur metabolic pathway in this bacterium.

A proposed model for thiosulfate oxidation metabolism in *H. thermophilus* is shown in the below Figure. At first, thiosulfate present in the culture medium is converted into insoluble sulfur species and sulfate by the sox system in the periplasm. Some of insoluble sulfur species are observed outside the cells as sulfur globules. The protein encoded by HTH_0586 was obtained from sulfur globules. This protein is a lipoprotein with seven tetratricopeptide repeat sequences, and is thought to be involved in release or uptake of sulfur globules while its detailed function is still unclear. It is believed that insoluble sulfur species are transported to cytoplasm as a low molecular persulfide compound. In cytoplasm, sulfite is produced by Hdr enzyme. Hdr is considered to perform enzymatic reaction by electron bifurcation mechanism, and persulfide, quinone, and GcvH protein are candidates of reaction partners. Sulfite produced in cytoplasm is oxidized to sulfate by SreABC. Electrons gained in each step are delivered to cytochrome *c* and quinone to obtain energy to grow.

Although physiological properties of enzymes for thiosulfate oxidation were shown in this study, to determine the reaction partners of Hdr and SreABC has not been successful. Also, enzymatic features of those proteins and HTH_0586 are not fully understood. Finally, I hope this study will help further development of sulfur metabolism researches.

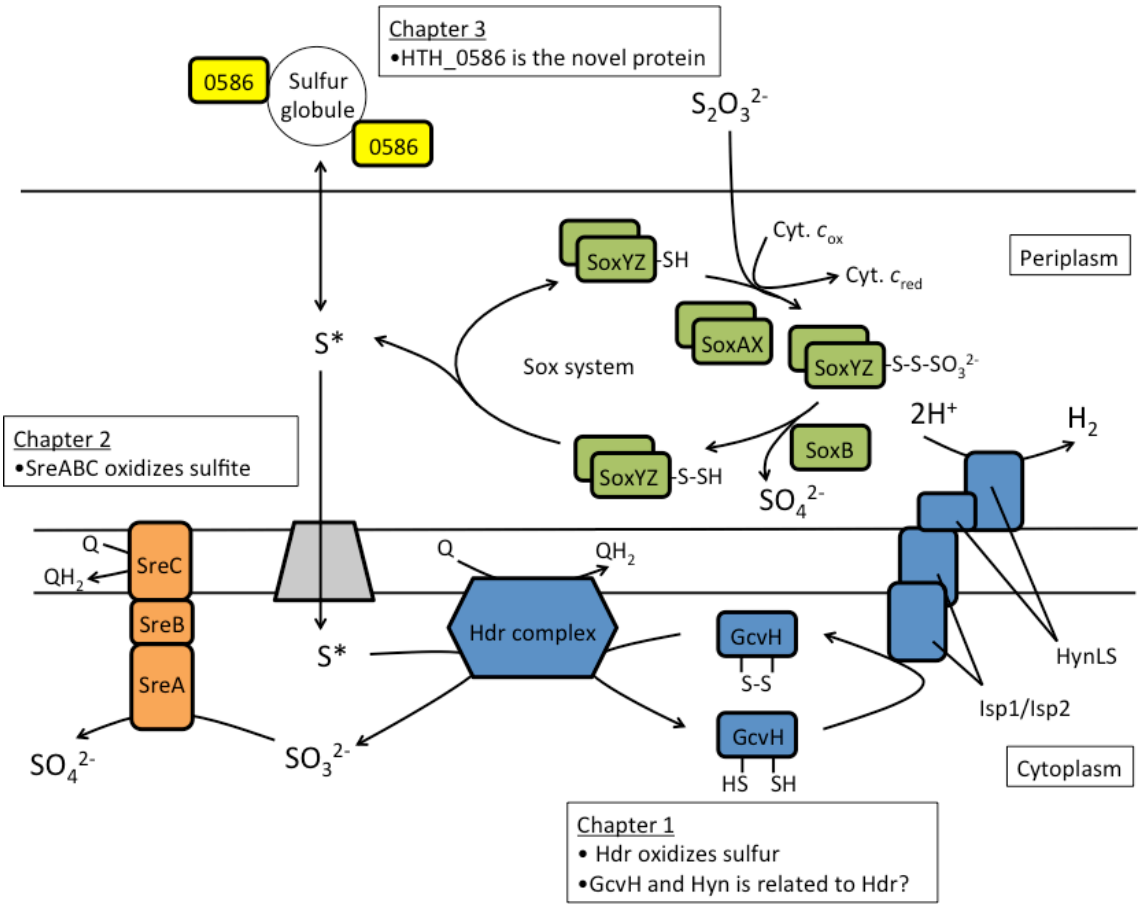

Fig. Simple overview of this study. Discussed enzymes in each chapter were represented by each color: blue, chapter 1; orange, chapter 2; yellow, chapter 3.

References

General introduction

(1) Garcia, A. A. Jr. and Druschel, G. K. (2014) Elemental sulfur coarsening kinetics, *Geochemical transactions*, **15**, 11.

(2) Maki, J. S. (2013) Bacterial intracellular sulfur globules: structure and function, *J. Mol. Microbiol. Biotechnol.*, **23**, 270-280.

(3) Kawasumi, T. *et. al.* (1980) Isolation of strictly thermophilic and obligately autotrophic hydrogen bacteria, *Agric. Biol. Chem.*, **44**, 1985-1986.

(4) Pitulle, C. *et. al.* (1994) Phylogenetic position of the genus *Hydrogenobacter*, *Int. J. Syst. Bacteriol.*, **44**, 620-626.

(5) Ishii, M. *et. al.* (1987) 2-Methylthio-1,4-naphtoquinone, a unique sulfur-containing quinone from thermophilic hydrogen-oxidizing bacterium, *Hydrogenobacter thermophilus*, *J. bacteriol.*, **169**, 2380-2384.

(6) Ishii, M. *et. al*. (1987) Purification and some properties of cytochrome c_{552} from *Hydrogenobacter thermophilus*, *Agric. Biol. Chem.*, **51**, 1695-1696.

(7) Ishii, M. *et. al.* (2000) Purification and characterization of membrane-bound hydrogenase from *Hydrogenobacter thermophilus* strain TK-6, an obligately autotrophic, thermophilic, hydrogen-oxidizing bacterium, *Biosci. Biotechnol. Biochem.*, **64**, 492-502.

(8) Yamamoto, M. *et. al.* (2003) Characterization of two different 2-oxoglutarate:ferredoxin oxidoreductases from *Hydrogenobater thermophilus* TK-6, *Biochem. Biophys. Res. Commun.*, **312**, 1297-1302.

(9) Ikeda, T. *et. al*. (2006) Anaerobic five subunit-type pyruvate:ferredoxin oxidoreductase from *Hydrogenobacter thermophilus* TK-6, *Biochem. Biophys. Res. Commun.*, **340**, 76-82.

(10) Aoshima, M., Ishii, M. and Igarashi, Y. (2004) A novel enzyme, citryl-CoA lyase, catalyzing the second step of the citrate cleavage reaction in *Hydrogenobacter thermophilus* TK-6, *Mol. Microbiol.*, **52**, 763-770.

(11) Aoshima, M. (2007) Novel enzyme reactions related to the tricaroxylic acid cycle: phylogenetic/functional implications and biotechnological applications, *Appl. Microbiol, Biotechnol*., **75**, 249-255.

(12) Miura, A. *et. al.* (2008) A soluble NADH-dependent fumarate reductase in the reductive tricarboxylic acid cycle of *Hydrogenobacter thermophilus* TK-6, *J. Bacteriol.*, **190**, 21, 7170-7177.

(13) Kameya, M. *et. al.* (2006) Purification and properties of glutamate synthetase from *Hydrogenobacter thermophilus* TK-6, *J. Biosci. Bioeng.*, **102**, 311-315.

(14) Kameya, M. *et. al.* (2007) A novel ferredoxin-dependent glutamate synthase from the hydrogen-oxidizing chemolithoautotrophic bacterium *Hydrogenobacter htermophilus* TK-6, *J. Bacteriol.*, **189**, 2805-2812.

(15) Kameya, M. *et. al.* (2017) Nitrate reductases in *Hydrogenobacter thermophilus* with evolutionarily ancient features: distinctive localization and electron transfer, *Mol. Microbiol.*, **106**, 1, 129-141.

(16) Chiba, Y. *et. al.* (2012) Crystallization and preliminary X-ray diffraction analysis of a novel type of phosphoserine phosphatase from *Hydrogenobacter thermophilus* TK-6, *Act. Cryst.*, **F68**, 911-913.

(17) Kim, K. *et. al.* (2016) Discovery of an intermolecular disulfide bond required for the thermostability of a heterodimeric protein from the thermophile *Hydrogenobacter thermophilus*, *Biosci. Biotechnol. Biochem.*, **80**, 2, 232-240.

(18) Sato, Y. *et. al.* (2011) A novel enzymatic systems against oxidative stress in the thermophilic hydrogen-oxidizing bacterium *Hydrogenobacter thermophilus*, *PLoS One*, **7**, e34825.

(19) Arai, H. *et. al.* (2010) Complete genome sequence of the thermophilic, obligately chemolithoautotrophic hydrogen-oxidizing bacterium *Hydrogenobacter thermophilus* TK-6, *J. Bacteriol.*, **192**, 2651-2652.

(20) Kawasumi, T. *et. al.* (1984) *Hydrogenobacter termophilus* gen. nol., sp. nov., an extremely thermophilic, aerobic, hydrogen-oxidizing bacterium, *Int. J. Syst. Bacteriol.*, **34**, 5-10.

(21) Bonjour, F. and Aragno, M. (1986) Growth of thermophilic, obilgately chemolithosutotrophic hydrogen-oxidizing bacteria related to *Hydrogenobacter* with thiosulfate and elemental sulfur as electron and energy source, *FEMS Microbiol. Lett.*, **35**, 11-15.

(22) Suzuki, M. *et. al.* (2001) Nitrate respiratory metabolism in an obligately

autotrophic hydrogen-oxidizing bacterium, *Hydrogenobacter thermophilus* TK-6, *Arch. Microbiol.*, **175**, 75-78.

(23) Shiba, H. *et. al.* (1985) The CO_2 assimilation via the reductive tricarboxylic acid cycle in an obligately autotrophic, aerobic hydrogen-oxidizing bacterium, *Hydrogenobacter thermophilus*, *Arch. Microbiol.*, **141**, 198-203.

(24) Yoshino, J *et. al.* (2001) Chemical structure of a novel aminophospholipid from *Hydrogenobacther thermophilus* strain TK-6, *J. Bacteriol.*, **183**, 6302-6304.

(25) Sano, R. *et. al.* (2010) Thiosulfate oxidation by a thermo-neutrophilic hydrogen-oxidizing bacterium, *Hydrogenobacter thermophilus*, *Biosci. Biotechnol. Biochem.,* **74**, 4, 892-894.

(26) Quatrini, R. *et. al.* (2009) Extending the models for iron and sulfur oxidation in the extreme acidophile *Acidithiobacillus ferrooxidans*, *BMC genomics*, **10**, 394.

(27) Dahl, C. *et. al.* (2013) Sulfite oxidation in the purple sulfur bacterium *Allochromatium vinosum*: identification of SoeABC as a major player and relevance of SoxYZ in the process, *Microbiology*, **159**, 2626-2638.

(28) Sato, Y. *et. al.* (2012) Transcriptome analyses for metabolic enzymes in thiosulfate- and hydrogen-grown *Hydrogenobacter thermophilus* cells, *Biosci. biotechnol. biochem.*, **76**, 9, 1677-1681.

(29) Wächtershäuser, G. (1990) Evolution of the first metabolic cycles, *Proc. Natl. Acad. Sci.*, **87**, 200-204.

(30) Ishizaki, M. (2014) Master thesis, The University of Tokyo.

Chapter 1-1

(1) Dahl, C. (2015) Cytoplasmic sulfur trafficking in sulfur-oxidizing prokaryotes, *IUBMB Life*, **67**, 4, 268-274.

(2) Auernik, K. S. and Kelly R. M. (2008) Identification of components of electron transport chains in the extremely thermoacidophilic Crearchaeon *Metallosphaera sedula* through iron and sulfur compound oxidation transcriptomes, *Appl. Environ. Microbial.*, **74**, 24, 7723-7732.

(3) Quatrini, R. *et. al.* (2009) Extending the models for iron and sulfur oxidation in the extreme acidophile *Acidithiobacillus ferrooxidans*, *BMC genomics*, **10**, 394.

(4) Thauer, R. K. *et. al.* (2008) Methanogenic archaea: ecologically relevant differences in energy conversion, *Nat. Rev. Microbiol.*, **6**, 579-591.

(5) Boughanemi, S. *et. al.* (2016) Microbial oxidative sulfur metabolism: biochemical evidence of the membrane-bound heterodisulfide reductase-like complex of the bacterium *Aquifex aeolicus*, *FEMS Microbiol. Lett.*, **363**, 15, fnw156.

(6) Shiba, H. *et. al.* (1982) The deficient carbohydrate metabolic pathway and the incomplete tricarboxylic acid cycle in an obligately autotrophic hydrogen-oxidizing bacterium, *Agric. Biol. Chem.*, **46**, 2341-2345.

(7) Ishizaki, M. (2014) Master thesis, The University of Tokyo.

(8) Dahl, C. (1996) Insertional gene inactivation in a phototrophic sulphur bacterium: APS-reductase-deficient mutants of *Chromatium vinosum*, *Microbiology*, **142**, 3363-3372.

(9) Schedel, M. and Trüper, H. G. (1980) Anaerobic oxidation of thiosulfate and elemental sulfur in *Thiobacillus denitrificans*, *Arch. Microbiol*., **124**, 205-210.

(10) Sörbo, B. (1987) Sulfate; turbidometric and nephelometric methods, *Methods Enyzmol*., **143**, 3-6.

(11) R Core Team (2015) R: A language and environment for statistical computing. R Foundation for Statistical Computing, Vienna, Austria. URL http://www.R-project.org/.

(12) Kannt, A. *et. al.* (1998) Electrical current generation and proton pumping catalyzed by the cytochrome *c* oxidase from *Thermus thermophilus*, *FEBS Lett.*, **434**, 17-22.

(13) Ludwig, B. (1980) Heme aa_3-type cytochrome *c* oxidase from bacteria, *Biochim. Biophys. Acta*, **594**, 177-189.

(14) Sato, Y. *et. al.* (2012) Transcriptome analyses for metabolic enzymes in thiosulfate- and hydrogen-grown *Hydrogenobacter thermophilus* cells, *Biosci. Biotechnol. Biochem.*, **76**, 9, 1677-1681.

(15) Tengölics, R. *et. al.* (2014) Connection between the membrane electron transport system and Hyn hydrogenase in the purple sulfur bacterium, *Thiocapsa roseopersicina* BBS, *Biochim. Biophys. Acta*, **1837**, 1691-1698.

(16) Welte, C. and Deppenmeier, U. (2011) Membrane-bound electron transport in

Methanosaeta thermophila, *J. Bacteriol.*, **193**, 11, 2868-2870.

(17) Palágyi-Mészáros, L. S. *et. al.* (2009) Electron-transfer subunits of the NiFe hydrogenases in *Thiocapsa roseopersicina* BBS, *FEBS J.*, **276**, 164-174.

Chapter 1-2

(1) Quatrini, R. *et. al.* (2009) Extending the models for iron and sulfur oxidation in the extreme acidophile *Acidithiobacillus ferrooxidans*, *BMC genomics*, **10**, 394.

(2) Liu, L. *et. al.* (2014) Thiosulfate transfer mediated by DsrE/TusA homologs from Acidothermophilic sulfur-oxidizing archaeon *Metallosphaera cuprina*, *J. Biol. Chem.*, **289**, 39, 26949-26959.

(3) Kikuchi, G. *et. al.* (2008) Glycine cleavage system: reaction mechanism, physiological significance, and hyperglycinemia, *Proc. Jpn. Acad. B.*, 84, 246-263.

(4) Sato, Y. *et. al.* (2012) Transcriptome analyses for metabolic enzymes in thiosulfate- and hydrogen-grown *Hydrogenobacter thermophilus* cells, *Biosci. Biotechnol. Biochem.*, **76**, 9, 1677-1681.

(5) Chiba, Y. (2012) Doctor thesis. The University of Tokyo.

(6) Peters, J. W. *et. al.* (2016) Electron bifurcation, *Curr. Opin. Chem. Biol.*, **31**, 146-152.

(7) Appel, A. M. *et. al.* (2013) Frontiers, opportunities, and challenges in biochemical and chemical catalysis of CO_2 fixation, *Chem. Rev.*, **133**, 8, 6621-6658.

(8) Costa, K. C. *et. al.* (2013) VhuD facilitates electron flow from H_2 or formate to heterodisulfide reductase in *Methanococcus maripaludis*, *J. Bacteriol.*, **195**, 22, 5160-5165.

(9) Boughanemi, S. *et. al.* (2016) Microbial oxidative sulfur metabolism: biochemical evidence of the membrane-bound heterodisulfide reductase-like complex of the bacterium *Aquifex aeolicus*, *FEMS Microbiol. Lett.*, **363**, 15, fnw156.

(10) Thauer, R. K., Jungermann, K, and Decker, K. (1977) Energy conservation in chemotrophic anaerobic bacteria, *Bacteriol. Rev.*, **41**, 1, 100-180.

(11) Roy, S. and Packer, L. (1998) Redox regulation of cell functions by α-lipoate: biochemical and molecular aspects, *BioFactors*, **7**, 263-267.

(12) Tengölics, R. *et. al.* (2014) Connection between the membrane electron transport system and Hyn hydrogenase in the purple sulfur bacterium, *Thiocapsa roseopersicina* BBS, *Biochim. Biophys. Acta*, **1837**, 1691-1698.

Chapter 2

(1) Kappler, U. and Dahl, C. (2001) Enzymology and molecular biology of prokaryotic sulfite oxidation, *FEMS Microbiol. Lett.*, **203**, 1-9.

(2) Robin, S. *et. al.* (2011) A sulfite respiration pathway from *Thermus thermophilus* and the key role of newly identified cytochrome c_{550}, *J. Bacteriol.*, **193**, 15, 3988-3997.

(3) Kappler, U. *et. al.* (2000) Sulfite:cytochrome *c* oxidoreductase from *Thiobacillus novellus*, purification, characterization, and molecular biology of a heterodimeric member of the sulfite oxidase family, *J. Biol. Chem.*, **278**, 18, 13202-13212.

(4) Yu, Z. *et. al.* (2007) Crystal structure of the bifunctional ATP sulfurylase – APS kinase from the chemolithoautotrophic thermophile *Aquifex aeolicus*, *J. Mol. Biol.*, **365**, 732-743.

(5) Sato, Y. *et. al.* (2012) Transcriptome analyses for metabolic enzymes in thiosulfate- and hydrogen-grown *Hydrogenobacter thermophilus* cells, *Biosci. Biotechnol. Biochem.*, **76**, 9, 1677-1681.

(6) Dahl, C. *et. al.* (2013) Sulfite oxidation in the purple sulfur bacterium *Allochromatium vinosum*: identification of SoeABC as a major player and relevance of SoxYZ in the process, *Microbiology*, **159**, 2626-2638.

(7) Dahl, C. (1996) Insertional gene inactivation in a phototrophic sulphur bacterium: APS-reductase-deficient mutants of *Chromatium vinosum*, *Microbiology*, **142**, 3363-3372.

(8) Burlage, R. S. *et. al.* (1998) Techniques in microbial ecology, pp. 45-46.

(9) Cohen, H. J. and Friedvich, I. (1971) Hepatic sulfite oxidase. The nature and function of the heme prosthetic groups, *J. Biol. Chem.*, **246**, 2, 367-373.

(10) Jormakka, M. (2002) Molecular basis of proton motive force generation: structure of formate dehydrogenase-N, *Science*, **295**, 1863-1868.

(11) Rothery, R. A., Workun, G. J. and Weiner, J. H. (2008) The prokaryotic complex

iron-sulfur molybdoenzyme family, *Biochem. Biophys. Acta*, **1778**, 1897-1929.

Chapter 3

(1) Inoue, T (2017) Master thesis, The University of Tokyo.

(2) Chen, L. *et. al.* (2012) *Acidithiobacillus caldus* sulfur oxidation model based on transcriptome analysis between the wild type and sulfur oxygenase reductase defective mutant, *PLoS ONE*, **7**, 9, e39470.

(3) Prange, A *et. al.* (2004) The role of the sulfur globule proteins of *Allochromatium vinosum*: mutagenesis of the sulfur globule protein genes and expression studies by real-time RT-PCR, *Arch. Microbial.*, **182**, 165-174.

(4) Brune, D. C. (1995) Isolation and characterization of sulfur globule proteins from *Chromatium vinosum* and *Thiocapsa roseopersicina*, *Arch. Microbiol.*, **163**, 391-399.

(5) Marnocha, C. L. *et. al.* (2016) Mechanisms of extracellular S^0 globules production and degradation in *Chlorobaculum tepidum* via dynamic cell-globule interaction, *Microbiology*, **162**, 1125-1134.

(6) Hanson, T. E. *et. al.* (2016) *Chlorobaculum tepidum* growth on biogenic S(0) as the sole photosynthetic electron donor, *Environ. Microbiol.*, **18**, 9, 2856-2867.

(7) Hirano, T. *et. al.* (1990) Snap helix with knob and hole: essential repeats in *S. pombe* nuclear protein nuc2+, *Cell*, **60**, 319-328.

(8) Sikorski, R. S. *et. al*. (1990) A repeating amino acid motif in CDC23 defines a family of proteins and a new relationship among genes required for mitosis and RNA synthesis, *Cell*, **60**, 307-317.

(9) Das, A. K., Cohen, P. T. W. and Barford, D (1998) The structure of the tetratricopeptide repeats of the protein phosphatase 5: implications for TPR-mediated protein-protein interactions, *EMBO J.*, **17**, 5, 1192-1199.

(10) Cerveny, L. *et. al.* (2013) Tetratricopeptide repeat motif in the world of bacterial pathogens: role in virulence mechanism, *Infect. Immun.*, **81**, 3, 629-635.

(11) Kim, K. *et. al.* (2006) Crystal structure of PilF: functional implication in the type 4 pilus biogenesis in *Pseudomonas aeruginosa*, *Biochem. Biophys. Research Commun.*, **340**, 1028-1038.

(12) Koo, J. *et. al.* (2008) PilF is an outer membrane lipoprotein required for multimerization and localization of the *Pseudomonas aeruginosa* type IV pilus secretin, *J. Bacteriol.*, **190**, 21, 6961-6969.

論文の内容の要旨

応用生命工学　専攻
平成２７年度博士課程　進学
氏　　名　小倉　一将
指導教員　石井　正治　教授

論文題目

The metabolism of thiosulfate in *Hydrogenobacter thermophilus* TK-6
(*Hydrogenobacter thermophilus* TK-6 のチオ硫酸代謝)

序章

硫黄は自然界で硫化物イオン (S^{2-})から硫酸イオン (SO_4^{2-})まで幅広い酸化状態を示し、炭素、水素、酸素、窒素などと並んで、生命活動に必須な元素の一つである。生体活動において硫黄はアミノ酸やビタミンに含まれる。また還元的な無機硫黄化合物は一部の進化的に古い真正細菌や古細菌のエネルギー源となることが知られており、初期生命の代謝においては硫黄がエネルギー源とされていた可能性が示唆されている。しかし、これらの生物の硫黄代謝に関する知見は少ないのが現状である。

Hydrogenobacter thermophilus TK-6 は真正細菌において最も早く分岐したと考えられている *Aquificales* に属する絶対独立栄養性の好熱性水素細菌である。これまでに本菌は、炭素代謝を始めとして多くの代謝が研究されており、その結果、特徴的な二酸化炭素固定経路である還元的 TCA サイクルや、進化的に古い可能性が示唆される数多くの新規酵素・代謝経路が発見されてきた。さらにゲノム解析は終了しており、本菌を用いた遺伝子操作技術が確立されていることから、代謝系を明らかにする上で強力なツールとなるオミックス解析、生理生化学的解析を行うことが可能である。

本菌は水素のみならず、チオ硫酸を唯一の電子源として利用することが可能である。本菌をチオ硫酸酸化条件で培養すると、培地中の pH の減少、硫黄由来の粒子の形成が確認される。さらに培養を続けると生成した硫黄粒子は減少していく。これらの現象と本菌のゲノム情報を比較することで、本菌はペリプラズムの Sox システムと呼ばれる代謝でチオ硫酸を硫酸と不溶性の硫黄化合物に酸化し、サイトプラズム内で生成した不溶性硫黄化合物をさらに酸化すると考えられた。

本菌において Sox システムに関わる酵素の研究は行われているが、サイトプラズムにおける硫黄の酸化機構は推測にとどまっていた。そこで本研究では、本菌における硫黄代謝に着目し、その全貌を明らかにすることを目的とした。第１章、第２章ではそれぞれ本菌のサイトプラズムにおける硫黄酸化酵素、亜硫酸酸化酵素に着目し、第３章においては、本菌が細胞外に生成する硫黄粒子に着目して研究を行った。

第１章　Sulfur-oxidizing enzyme

第１節　Physiological analysis of sulfur-oxidizing gene

硫黄を酸化する真正細菌、古細菌のトランスクリプトーム解析によって、Heterodisulfide reductase (Hdr)-like enzyme がサイトプラズム内での硫黄の酸化を行うことが示唆されてきた。Hdr はメタン生成菌において初めて同定された酵素で、メタン生成経路の最終ステップにおいて CoM-S-S-CoB のジスルフィド結合を開裂する反応を触媒する酸化還元酵素である。Hdr を有する真正細菌では、元素硫黄をエネルギー源とした際にこの遺伝子群の発現レベルが上昇することから、メタン生成菌の Hdr とは全く異なる、硫黄の酸化反応を触媒するのではないかと示唆されてきた。一方で、本遺伝子の生理学的知見は得られてこなかった。そこで遺伝子破壊株を作製し、その表現型の解析を行った。

その結果、*hdrA* 破壊株 (Δ*hdrA*)は野生株と比較して、生育が非常に悪くなった。チオ硫酸の消費速度は変化がなかったが、培地中の硫酸量が約半分になった。また pH の変化も見られなくなった。さらに変異株では培養液中の元素硫黄量が増加し、培養後期においても、全ての元素硫黄は酸化されなかった。従って、*hdrA* は生体内で硫黄の酸化と、チオ硫酸からのエネルギー獲得に重要な働きをすることが示唆された。

Hdr と機能的に関連する遺伝子を調べるために、マイクロアレイ解析を行った。野生株とΔ*hdrA* をチオ硫酸存在下で培養し、遺伝子発現プロファイルを比較した。

その結果、特に呼吸関連遺伝子について大きな発現レベルの変動が見られ、Δ*hdrA* では、エネルギーをより効率的に利用しようとする傾向が見られた。また、Δ*hdrA* では一部のヒドロゲナーゼの発現レベルが低下したことから、Hdr とヒドロゲナーゼの機能的関連が示唆された。

第２節　Functional analyses of glycine cleavage system genes present in *hdr* cluster

hdr クラスターは比較的大きな遺伝子クラスターであり、真正細菌では Hdr 複合体のサブユニット以外にも保存された遺伝子が存在する。グリシン開裂系の H タンパク質である *gcvH* も *hdr* クラスター中に保存された遺伝子の一つである。本菌が持つ *hdr* クラスター中の *gcvH* (*gcvH3* および *gcvH4*)は構成的に発現しているのにも関わらず、グリシン開裂系の酵素活性は検出されていない。そこで、*gcvH3* および *gcvH4* を異種発現し、その機能を調べた。2 つの GcvH と相互作用するタンパク質を本菌の可溶画分中、膜画分中から探索したが、相互作用の力が弱かったためか、タンパク質を同定することはできなかった。

第２章　Sulfite-oxidizing enzyme

亜硫酸は主要な硫黄の酸化過程で生じる主要な中間体である。亜硫酸は強い還元力を有するため、DNA やタンパク質と容易に反応して毒性を発揮する。そのため生物は亜硫酸に対する解毒メカニズムをそれぞれ持っている。本菌ではペリプラズムに亜硫酸酸化酵素が存在することは知られていた。しかし硫黄の酸化はサイトプラズム内で行われることから、サイトプラズムに局在する亜硫酸酸化酵素の存在が示唆された。本菌の SreABC は光合成細菌において近年発見された新規な亜硫酸酸化酵素と相同性を持っていた。そこで本研究では、主に SreABC に着目し、本菌の持つ亜硫酸酸化酵素についての解析を行った。

始めに *sreA* の遺伝子破壊株 (Δ*sreA*)を作製し、その表現型を観察した。Δ*sreA* は野生株と比較して、培養液中により多くの亜硫酸の蓄積が見られたことから、本菌の *sreA* は *in vivo* で亜硫酸酸化酵素として機能することが示唆された。本菌の膜画分を用いて、SreABC による亜硫酸酸化酵素の測定を試みた。複数種の活性測定系を検討したが、酵素活性を測定することはできなかった。ペリプラズムにおける亜硫酸酸化酵素の活性が測定され、Δ*sreA* においてはより強い活性が見られた。

第３章　Sulfur globule

本菌はチオ硫酸を電子源とした際に、菌体外に硫黄由来の粒子を形成する。このような現象は一部の光合成細菌においても確認されており、その性質が研究されている。しかし本菌のような好熱性細菌では、硫黄粒子の研究は進んでいない。そこで本章では、本菌が生成する硫黄粒子に着目して研究を行った。本菌をチオ硫酸存在下で培養し、スクロース溶液中を通すことで菌体と硫黄粒子を分画した。ゼータサイザーによって硫黄粒子の粒子径を測定した結果、3

種類の粒子径（約 70 nm, 約 300 nm, 約 2 μm）が得られた。　SDS-PAGE によって、硫黄粒子中に特有のタンパク質が存在するか調べた。その結果、明らかに硫黄粒子特有のタンパク質が確認され、プロテインシーケンサーによってタンパク質が同定された。このタンパク質は既知の硫黄粒子関連タンパク質とは相同性のない新規なものであった。

総括

以下の図に示すような、*H. thermophilus* におけるチオ硫酸酸化代謝を提唱した。各遺伝子の生理学的な役割を推察することができた。

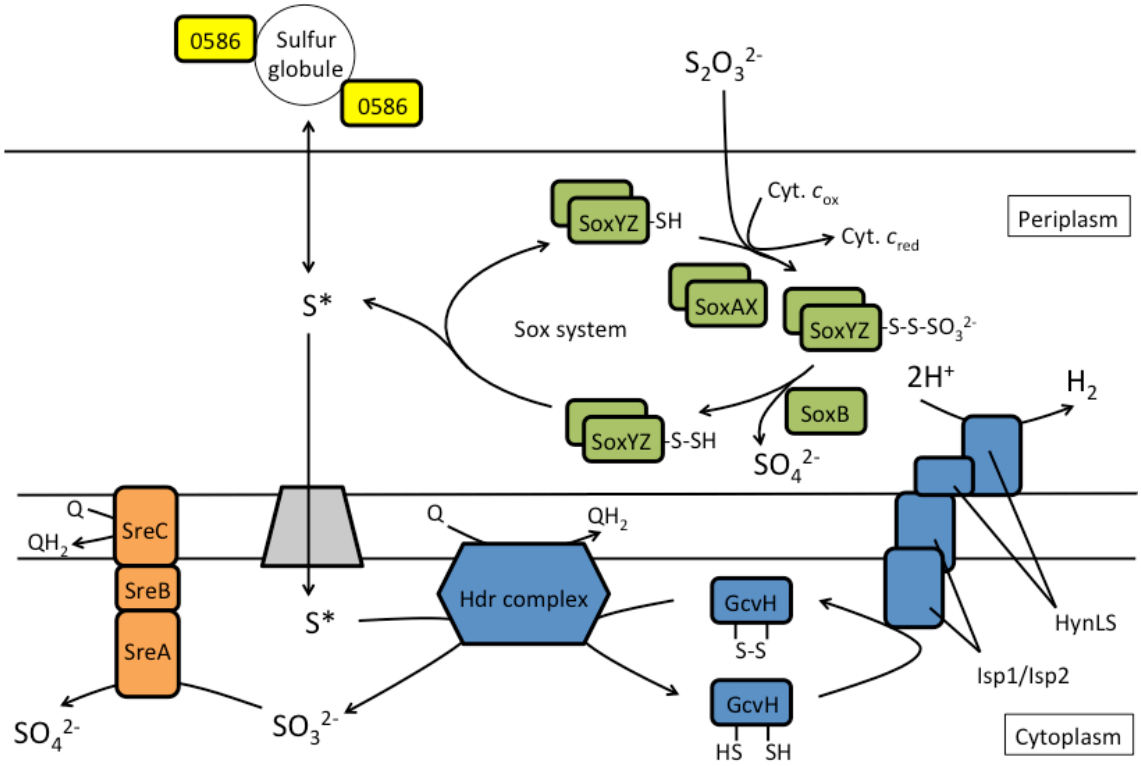

Fig. *H. thermophilus* TK-6 のチオ硫酸代謝

Appendix

Table S1 Up-regulated genes in Δ*hdrA* (more than 3-fold changes)

Cellular processes and signaling		
[D] Cell cycle control, cell division, chromosome partitioning		
Locus tag	Description	Fold change ([dHdrA]/[WT])
HTH_1068	septum site-determining protein	3.71
HTH_1069	cell division topological specificity factor	4.14
[M] Cell wall/membrane/envelope biogenesis		
Locus tag	Description	Fold change ([dHdrA]/[WT])
HTH_0600	UTP-glucose-1-phosphate uridylyltransferase	8.69
HTH_1189	ABC transporter	6.22
HTH_1749	hypothetical protein	5.15
[N] Cell motility		
Locus tag	Description	Fold change ([dHdrA]/[WT])
HTH_0255	general secretion pathway protein G	4.20
[O] Post-translational modification, protein turnover, and chaperones		
Locus tag	Description	Fold change ([dHdrA]/[WT])
HTH_0110	hypothetical protein	4.00
HTH_0385	xanthine and CO dehydrogenase maturation factor, XdhC/CoxF family	3.63
HTH_0583	thioredoxin-like protein	8.37
HTH_0695	33 kDa chaperonin	3.05
HTH_0775	hypothetical protein	3.40
HTH_1042	SirA family protein	4.18
HTH_1104	cytochrome c peroxidase	4.91
HTH_1194	SCO1/SenC/PrrC family protein	3.58
HTH_1262	heat shock protein	4.00

HTH_1351	thiol:disulfide interchange protein	3.38
HTH_1399	band 7 protein	3.53
HTH_1556	carboxyl-terminal protease	3.00
HTH_1567	putative zinc metalloprotease	4.01
HTH_1663	iron-sulfur cluster assembly accessory protein	4.27
HTH_1793	10 kDa chaperonin GroES	4.00
HTH_1846	thioredoxin reductase	4.19
HTH_1886	SirA family protein	3.86
[T] Signal transduction mechanisms		
Locus tag	Description	Fold change ([dHdrA]/[WT])
HTH_0036	diguanylate cyclase/phosphodiesterase	3.84
HTH_0442	sigma 54 dependent transcriptional regulator	3.25
HTH_0967	sensor protein	7.00
HTH_0968	transcriptional regulator, NtrC family	3.10
HTH_1119	nitrogen regulatory protein PII	4.76
HTH_1120	nitrogen regulatory protein PII	4.45
HTH_1481	hemerythrin-like metal-binding protein	3.07
HTH_1549	sensor histidine kinase	3.32
HTH_1560	cyclic nucleotide-binding protein	6.64
HTH_1620	transcriptional regulator, Crp/Fnr family	3.55
HTH_1766	scriptional regulator, Crp/Fnr family	3.93
[U] Intracellular trafficking, secretion, and vesicular transport		
Locus tag	Description	Fold change ([dHdrA]/[WT])
HTH_1677	biopolymer transport protein	5.55
[V] Defense mechanisms		
Locus tag	Description	Fold change ([dHdrA]/[WT])
HTH_0015	type I restriction-modification system R subunit	6.18
HTH_0018	restriction endonuclease S subunit	3.41

HTH_0019	type I restriction-modification system methyltransferase subunit	5.23
HTH_1249	CRISPR-associated protein	6.07
Information storage and processing		
[J] Translation, ribosomal structure and biogenesis		
Locus tag	Description	Fold change ([dHdrA]/[WT])
HTH_0280	peptide deformylase	5.62
HTH_0309	DnaK suppressor protein	5.31
HTH_0570	poly A polymerase	3.07
HTH_0759	translation initiation factor 3	6.29
HTH_0779	GTP cyclohydrolase I family protein	5.34
HTH_0820	ribosomal protein S20	10.82
HTH_0949	D-tyrosyl-tRNA(Tyr) deacylase	3.81
HTH_0987	16S rRNA processing protein RimM	4.37
HTH_1161	queuosine biosynthesis protein	3.72
HTH_1202	ribosomal-protein-alanine acetyltransferase	8.09
HTH_1839	tRNA modification GTPase	5.55
[K] Transcription		
Locus tag	Description	Fold change ([dHdrA]/[WT])
HTH_0501	cold shock protein	6.74
HTH_0997	DNA-directed RNA polymerase omega subunit	3.10
HTH_1135	Nif-specific regulatory protein	4.64
HTH_1816	transcriptional regulator, TetR family	3.26
HTH_1838	transcription termination factor Rho	9.83
[L] Replication, recombination and repair		
Locus tag	Description	Fold change ([dHdrA]/[WT])
HTH_0251	DNA repair protein RecN	3.69
HTH_0784	DNA replication protein DnaC	7.87
HTH_0805	ATP-dependent RNA helicase	4.76

HTH_1748	integration host factor beta subunit	4.27
Metabolism		
[C] Energy production and conversion		
Locus tag	Description	Fold change ([dHdrA]/[WT])
HTH_0119	NADH dehydrogenase I chain E	3.52
HTH_0384	carbon monoxide dehydrogenase subunit G	5.74
HTH_0386	carbon monoxide dehydrogenase middle subunit	6.29
HTH_0387	carbon monoxide dehydrogenase large subunit	7.94
HTH_0388	carbon monoxide dehydrogenase small subunit	31.55
HTH_0456	Ni,Fe-hydrogenase small subunit	3.59
HTH_0498	NADH ubiquinone oxidoreductase 20 kDa subunit/hydrogenase	3.41
HTH_0776	phosphoglycolate phosphatase	3.04
HTH_0817	sulfide dehydrogenase flavoprotein subunit	23.42
HTH_0875	cytochrome c biogenesis protein	3.07
HTH_0965	oxido/reductase iron sulfur protein	4.10
HTH_0983	fumarate reductase subunit B	5.50
HTH_1095	2-oxoglutarate:ferredoxin oxidoreductase alpha subunit	3.64
HTH_1116	assimilatory nitrite reductase	3.67
HTH_1469	nitroreductase	31.59
HTH_1553	pyruvate:ferredoxin oxidoreductase alpha subunit	3.12
HTH_1555	pyruvate:ferredoxin oxidoreductase epsilon subunit	12.40
HTH_1680	NAD-dependent formate dehydrogenase gamma subunit	9.35
HTH_1684	uncharacterized protein required for formate dehydrogenase activity	5.87
HTH_1737	citryl-CoA synthetase large subunit	3.49
HTH_1747	geranylgeranyl reductase	4.11
HTH_1863	fumarate reductase subunit E	8.21
[E] Amino acid transport and metabolism		
Locus tag	Description	Fold change ([dHdrA]/[WT])
HTH_0076	anthranilate synthase component II	6.71
HTH_0376	acetyltransferase	3.28

HTH_0403	ABC-type branched-chain amino acid transport system ATPase component	3.24
HTH_0682	S-adenosylmethionine decarboxylase proenzyme	4.02
HTH_0750	translation initiation factor 2B subunit I family	5.55
HTH_0874	imidazole glycerol phosphate synthase glutamine amidotransferase subunit	4.52
HTH_1160	ornithine decarboxylase	6.76
HTH_1395	glycine oxidase	3.59
HTH_1535	glycine cleavage system H protein	3.05
HTH_1536	glycine dehydrogenase (decarboxylating)	3.40
HTH_1581	pyrroline carboxylate reductase	6.34
HTH_1832	glycine/serine hydroxymethyltransferase	3.95
[F] Nucleotide transport and metabolism		
Locus tag	Description	Fold change ([dHdrA]/[WT])
HTH_0873	orotidine 5'-phosphate decarboxylase	3.36
HTH_1070	HAD-superfamily subfamily IIA hydrolase-like protein	4.15
HTH_1588	HAD-superfamily hydrolase	6.55
HTH_1771	phosphoribosylaminoimidazole-succinocarboxamide synthase	3.75
[G] Carbohydrate transport and metabolism		
Locus tag	Description	Fold change ([dHdrA]/[WT])
HTH_0038	1,4-alpha-glucan branching enzyme	3.08
HTH_0107	3-phosphoglycerate kinase	2.19
HTH_0117	transketolase	3.49
HTH_0611	triosephosphate isomerase	2.27
HTH_0868	ribose 5-phosphate isomerase B	2.88
HTH_1035	ABC-type transporter permease component	2.18
HTH_1566	transaldolase	2.96
HTH_1639	O-antigen export system permease protein	2.08
HTH_1640	O-antigen export system ATP-binding protein	3.95

[H] Coenzyme transport and metabolism		
Locus tag	Description	Fold change ([dHdrA]/[WT])
HTH_0199	thiamine biosynthesis protein	3.87
HTH_0607	molybdenum cofactor biosynthesis protein A	4.91
HTH_0668	aspartate 1-decarboxylase	5.06
HTH_0739	molybdopterin converting factor small subunit	4.97
HTH_0818	thiamine monophosphate synthase	10.51
HTH_0977	molybdenum cofactor biosynthesis protein	3.91
HTH_1048	biotin/lipoate A/B protein ligase	4.74
HTH_1087	GTP cyclohydrolase I	9.24
HTH_1185	molybdopterin-converting factor subunit 2	3.45
HTH_1212	coenzyme PQQ synthesis protein C	51.15
HTH_1214	coenzyme PQQ synthesis protein C	20.58
HTH_1238	radical SAM domain protein	3.66
HTH_1271	lipoate protein ligase	3.14
HTH_1272	biotin synthase	3.06
HTH_1329	molybdopterin-guanine dinucleotide biosynthesis protein A	4.91
HTH_1382	molybdopterin converting factor small subunit	3.23
HTH_1563	thiamine biosynthesis protein	6.87
HTH_1603	lipoate-protein ligase A	3.94
HTH_1666	dihydropteroate synthase	3.57
HTH_1842	uroporphyrinogen-III synthetase	6.31
[I] Lipid transport and metabolism		
Locus tag	Description	Fold change ([dHdrA]/[WT])
HTH_0004	short-chain dehydrogenase	3.13
HTH_0077	acyl-coenzyme A synthetase	3.22
HTH_0217	putative sterol carrier protein	22.67
HTH_0325	phosphatidylglycerophosphatase A	4.63
HTH_0631	(3R)-hydroxymyristoyl-(acyl-carrier-protein) dehydratase	3.01
HTH_0837	cyclopropane-fatty-acyl-phospholipid synthase	4.62
HTH_0936	putative CoA-substrate-specific enzyme activase	5.27

HTH_1772	long-chain fatty acid transport protein	7.01
[P] Inorganic ion transport and metabolism		
Locus tag	Description	Fold change ([dHdrA]/[WT])
HTH_0057	cyanoglobin family protein	4.17
HTH_0389	TonB-dependent siderophore receptor	3.68
HTH_0451	nitrogen-fixing NifU-like protein	3.27
HTH_1040	DsrE-like protein	3.15
HTH_1215	coenzyme PQQ synthesis protein B	3.54
HTH_1583	cation efflux system protein	4.07
HTH_1586	ammonium transporter	10.15
HTH_1596	rhodanese domain protein	4.35
HTH_1615	transcriptional regulator, Fur family	3.59
[R] General function prediction only		
Locus tag	Description	Fold change ([dHdrA]/[WT])
HTH_0017	nucleotidyltransferase	6.07
HTH_0020	MoxR-like ATPase	3.50
HTH_0035	beta-lactamase-like protein	5.11
HTH_0073	intracellular protease	4.65
HTH_0106	putative carbonic anhydrase/acetyltransferase	4.54
HTH_0235	putative dioxygenase	4.71
HTH_0290	DNA polymerase beta-like region/nucleotidyltransferase	10.07
HTH_0299	beta-lactamase-like protein	3.78
HTH_0391	conserved hypothetical protein	39.54
HTH_1107	conserved hypothetical protein	3.61
HTH_1213	coenzyme PQQ synthesis protein E	20.90
HTH_1331	endonuclease III	3.19
HTH_1480	hypothetical protein	3.37
HTH_1522	beta-lactamase-like protein	8.29
HTH_1636	2-nitropropane dioxygenase	5.57
HTH_1682	NAD-dependent formate dehydrogenase alpha subunit	5.86

HTH_1695	radical SAM domain protein	5.39
HTH_1797	hypothetical protein	3.13
HTH_1884	hypothetical protein	3.43
[S] Function unknown		
Locus tag	Description	Fold change ([dHdrA]/[WT])
HTH_0321	hypothetical protein	3.32
HTH_1086	conserved hypothetical protein	12.09
HTH_1515	sulfur oxidation protein	6.25
HTH_1521	hypothetical protein	6.73
HTH_1562	conserved hypothetical protein	15.79
HTH_1887	hypothetical protein	3.44
Others		
Locus tag	Description	Fold change ([dHdrA]/[WT])
HTH_0016	hypothetical protein	6.60
HTH_0050	hypothitical protein	3.47
HTH_0052	hypothetical protein	8.50
HTH_0058	hypothetical protein	4.11
HTH_0080	hypothetical protein	5.44
HTH_0133	hypothetical protein	5.38
HTH_0216	hypothetical protein	4.31
HTH_0248	hypothetical protein	4.66
HTH_0249	hypothetical protein	3.52
HTH_0254	hypothetical protein	7.81
HTH_0274	hypothetical protein	4.68
HTH_0279	hypothetical protein	5.28
HTH_0289	putative bacteriophage protein	4.87
HTH_0381	hypothetical protein	7.48
HTH_0382	hypothetical protein	8.22
HTH_0395	hypothetical protein	5.18
HTH_0432	DNA polymerase III gamma/tau subunit	3.62

HTH_0437	hypothetical protein	3.47
HTH_0449	hypothetical protein	3.72
HTH_0457	hypothetical protein	3.66
HTH_0471	hypothetical protein	3.00
HTH_0523	hypothetical protein	12.08
HTH_0524	hypothetical protein	3.83
HTH_0536	hypothetical protein	3.09
HTH_0605	hypothetical protein	3.07
HTH_0645	nucleotidyltransferase substrate binding protein	7.00
HTH_0646	hypothetical protein	7.94
HTH_0669	hypothetical protein	4.18
HTH_0778	hypothetical protein	11.32
HTH_0783	hypothetical protein	3.36
HTH_0794	hypothetical protein	5.90
HTH_0798	hypothetical protein	4.68
HTH_0799	hypothetical protein	3.77
HTH_0872	hypothetical protein	3.72
HTH_0896	hypothetical protein	3.99
HTH_0903	hypothetical protein	3.31
HTH_0906	hypothetical protein	3.23
HTH_0907	hypothetical protein	4.62
HTH_0908	hypothetical protein	4.31
HTH_0909	hypothetical protein	4.21
HTH_0911	DNA-binding excisionase-like protein	8.66
HTH_0941	hypothetical protein	3.25
HTH_0948	hypothetical protein	4.38
HTH_0994	putative lipoprotein	9.13
HTH_1067	septum site-determining protein	3.57
HTH_1084	hypothetical protein	5.52
HTH_1089	hypothetical protein	4.03
HTH_1094	2-oxoglutarate:ferredoxin oxidoreductase delta subunit	5.19
HTH_1117	hypothetical protein	3.94
HTH_1118	periplasmic transport protein	5.05
HTH_1147	hypothetical protein	5.03
HTH_1163	hypothetical protein	3.49

HTH_1186	hypothetical protein	3.02
HTH_1190	hypothetical protein	9.90
HTH_1191	hypothetical protein	3.77
HTH_1201	hypothetical protein	7.55
HTH_1210	hypothetical protein	3.43
HTH_1248	CRISPR-associated protein	5.15
HTH_1250	CRISPR-associated protein	4.93
HTH_1359	hypothetical protein	5.59
HTH_1372	hypothetical protein	3.15
HTH_1380	hypothetical protein	4.76
HTH_1384	hypothetical protein	5.05
HTH_1389	hypothetical protein	8.85
HTH_1390	hypothetical protein	5.55
HTH_1447	hypothetical protein	5.13
HTH_1463	cytochrome c, class I	6.36
HTH_1482	hypothetical protein	5.06
HTH_1512	nicotinate (nicotinamide) nucleotide adenylyltransferase	3.69
HTH_1514	thioredoxin	18.58
HTH_1516	sulfur oxidation protein	4.95
HTH_1548	response regulator	5.16
HTH_1554	pyruvate:ferredoxin oxidoreductase delta subunit	7.14
HTH_1587	hypothetical protein	5.41
HTH_1629	hypothetical protein	4.75
HTH_1635	hypothetical protein	4.02
HTH_1637	hypothetical protein	3.59
HTH_1660	hypothetical protein	4.37
HTH_1661	hypothetical protein	5.47
HTH_1662	hypothetical protein	5.28
HTH_1664	hypothetical protein	5.66
HTH_1678	biopolymer transport protein	6.45
HTH_1679	hypothetical protein	5.39
HTH_1683	NAD-dependent formate dehydrogenase delta subunit	10.38
HTH_1698	hypothetical protein	7.29
HTH_1782	hypothetical protein	3.83
HTH_1801	hypothetical protein	5.12

HTH_1804	hypothetical protein	3.43
HTH_1820	hypothetical protein	4.91
HTH_1822	putative endonuclease	3.22
HTH_1847	hypothetical protein	4.45
HTH_1862	hypothetical protein	3.41

Table S1 Down-regulated genes in Δ*hdrA* (more than 3-fold changes)

Cellular processes and signaling		
[D] Cell cycle control, cell division, chromosome partitioning		
Locus tag	Description	Fold change (-[WT]/[dHdrA])
HTH_1158	ATP/GTP-binding protein	-4.11
[M] Cell wall/membrane/envelope biogenesis		
Locus tag	Description	Fold change (-[WT]/[dHdrA])
HTH_0029	outer membrane efflux protein	-8.37
HTH_0032	efflux transporter	-3.07
HTH_0366	UDP-glucose 6-dehydrogenase	-4.80
HTH_0787	lipoprotein signal peptidase	-4.20
HTH_0938	ABC transporter ATP-binding protein	-10.17
HTH_1377	inner membrane protein	-3.35
HTH_1507	outer membrane efflux protein	-16.00
HTH_1508	cation efflux system	-32.24
HTH_1693	heavy metal efflux pump, CzcB family	-36.40
HTH_1694	heavy metal resistance protein	-31.05
HTH_1805	outer membrane efflux protein	-4.06
[N] Cell motility		
Locus tag	Description	Fold change (-[WT]/[dHdrA])
HTH_0269	glycosyltransferase	-4.29
HTH_0428	type II secretion system protein E	-9.89
HTH_1444	type IV pilus assembly protein	-6.15

[O] Post-translational modification, protein turnover, and chaperones		
Locus tag	Description	Fold change (-[WT]/[dHdrA])
HTH_0490	ADP-ribosylglycohydrolase	-3.60
HTH_1487	SCO1/SenC/PrrC family protein	-5.13
HTH_1714	putative nitrate reductase subunit	-4.35
[T] Signal transduction mechanisms		
Locus tag	Description	Fold change (-[WT]/[dHdrA])
HTH_0470	histidine kinase sensor protein	-4.28
HTH_1498	universal stress protein	-3.15
HTH_1504	two component transcriptional regulator	-4.01
HTH_1505	two-component sensor His kinase	-8.11
HTH_1689	two-component response regulator	-10.41
[U] Intracellular trafficking, secretion, and vesicular transport		
Locus tag	Description	Fold change (-[WT]/[dHdrA])
HTH_0100	biopolymer transport protein ExbD/TolR-type	-6.56
HTH_0101	biopolymer transport protein ExbB/TolQ-type	-7.17
HTH_0722	preprotein translocase SecY subunit	-5.62
HTH_1432	gliding motility protein	-3.32
[V] Defense mechanisms		
Locus tag	Description	Fold change (-[WT]/[dHdrA])
HTH_0028	multidrug resistance efflux pump	-8.65
HTH_0159	NosF protein	-6.06
HTH_0939	periplasmic component of efflux system	-31.36
Information storage and processing		

[J] Translation, ribosomal structure and biogenesis		
Locus tag	Description	Fold change (-[WT]/[dHdrA])
HTH_0061	SAM dependent methyl transferase	-5.15
HTH_0174	lysyl-tRNA synthetase	-3.26
HTH_0304	GTP-binding protein	-4.28
HTH_0719	ribosomal protein L18	-3.75
HTH_0720	ribosomal protein L30	-3.05
HTH_0721	ribosomal protein L15	-3.56
HTH_0724	methionine aminopeptidase	-4.21
HTH_0725	translation initiation factor 1	-4.95
HTH_0841	isoleucyl-tRNA synthetase	-4.02
HTH_0845	ribosomal protein S3	-4.32
HTH_0847	ribosomal protein S19	-4.36
HTH_0848	ribosomal protein L2	-4.34
HTH_0849	ribosomal protein L23	-6.13
HTH_0850	ribosomal protein L4	-5.79
HTH_0851	ribosomal protein L3	-4.18
HTH_0852	ribosomal protein S10	-3.00
HTH_0854	elongation factor EF-G	-4.81
HTH_0855	ribosomal protein S7	-5.49
HTH_0856	ribosomal protein S12	-4.09
HTH_0860	ribosomal protein L10	-4.23
HTH_1176	polyribonucleotide nucleotidyltransferase	-4.92
HTH_1368	translation factor SUA5 protein	-3.67
HTH_1815	hydrogenase maturation factor	-4.95
[K] Transcription		
Locus tag	Description	Fold change (-[WT]/[dHdrA])
HTH_0365	exoribonuclease R	-4.96
HTH_0857	DNA-directed RNA polymerase beta' subunit	-7.89
[L] Replication, recombination and repair		

Locus tag	Description	Fold change (-[WT]/[dHdrA])
HTH_0122	phage SPO1 DNA polymerase-related protein	-4.75
HTH_0514	resolvase domain protein	-6.34
HTH_0530	ATP-dependent DNA helicase	-6.28
HTH_1293	single-strand-DNA-specific exonuclease	-3.05
HTH_1448	ribonuclease HII	-4.26
Metabolism		
[C] Energy production and conversion		
Locus tag	Description	Fold change (-[WT]/[dHdrA])
HTH_0094	Fe-S oxidoreductase	-8.58
HTH_0095	Ni,Fe-hydrogenase large subunit	-4.65
HTH_0153	heme/copper-type cytochrome/quinol oxidase subunit 1	-7.24
HTH_0154	heme/copper-type cytochrome/quinol oxidase subunit 2	-4.30
HTH_0156	cytochrome b/b6	-10.67
HTH_0410	NADH dehydrogenase chain L	-6.40
HTH_0411	NADH dehydrogenase chain M	-3.58
HTH_0632	cytochrome c	-33.41
HTH_0930	formate dehydrogenase beta subunit	-26.53
HTH_0931	formate dehydrogenase gamma subunit	-19.33
HTH_0933	formate dehydrogenase formation protein FdhE	-25.65
HTH_0988	cytochrome c-552	-8.34
HTH_1058	nitroreductase	-4.46
HTH_1061	aldehyde dehydrogenase	-6.27
HTH_1062	membrane-bound aldehyde dehydrogenase small subunit	-4.72
HTH_1063	NADH:flavin oxidoreductase/NADH oxidase	-3.41
HTH_1152	formate hydrogenlyase subunit 4/respiratory-chain NADH dehydrogenase subunit 1	-4.23
HTH_1333	ubiquinol-cytochrome c reductase cytochrome b subunit	-4.08
HTH_1392	2-oxoglutarate carboxylase large subunit	-3.02
HTH_1486	cytochrome c oxidase subunit I	-5.03
HTH_1716	nitrate reductase beta subunit	-21.08

HTH_1787	NADH dehydrogenase I chain N	-4.48
HTH_1788	NADH dehydrogenase I chain M	-10.87
HTH_1789	NADH dehydrogenase I chain L	-6.64
HTH_1878	heterodisulfide reductase subunit B	-4.40
HTH_1879	heterodisulfide reductase subunit C	-5.89
[E] Amino acid transport and metabolism		
Locus tag	Description	Fold change (-[WT]/[dHdrA])
HTH_0008	aminotransferase	-8.50
HTH_0104	aminotransferase, class V	-3.01
HTH_0357	aminotransferase	-3.77
HTH_0532	phosphoadenosine phosphosulfate reductase	-10.21
HTH_0639	leucine aminopeptidase	-3.07
HTH_0664	prephenate dehydrogenase	-7.67
HTH_0934	glycine cleavage system protein H	-38.77
HTH_1367	threonine synthase	-4.69
HTH_1378	selenide, water dikinase/selenophosphate synthase	-6.78
HTH_1610	transporter (extracellular solute binding protein family 5)	-9.75
HTH_1877	glycine cleavage system H protein	-5.03
[F] Nucleotide transport and metabolism		
Locus tag	Description	Fold change (-[WT]/[dHdrA])
HTH_0084	NAD(+) kinase	-4.04
HTH_0663	dihydroorotase	-5.84
HTH_0723	adenylate kinase	-7.41
HTH_0786	phosphoribosylformylglycinamidine synthase II	-3.81
HTH_1420	phosphoribosylaminoimidazole carboxylase ATPase subunit	-4.25
HTH_1455	CTP synthetase	-3.05
HTH_1872	nucleoside-triphosphatase	-5.59
[G] Carbohydrate transport and metabolism		

Locus tag	Description	Fold change (-[WT]/[dHdrA])
HTH_0010	putative aldolase	-3.15
HTH_0087	glucan phosphorylase	-5.88
HTH_0088	glucan phosphorylase	-5.15
HTH_0103	phosphoglycerate mutase	-4.44
HTH_0275	4-alpha-glucanotransferase	-7.02
HTH_1612	KpsF/GutQ family protein	-6.44
[H] Coenzyme transport and metabolism		
Locus tag	Description	Fold change (-[WT]/[dHdrA])
HTH_0096	biotin-(acetyl-CoA carboxylase) ligase	-6.33
HTH_0613	4-hydroxybenzoate octaprenyltransferase	-4.42
HTH_1346	aminotransferase	-3.03
HTH_1909	hypothetical protein	-3.24
[I] Lipid transport and metabolism		
Locus tag	Description	Fold change (-[WT]/[dHdrA])
HTH_0009	enoyl-[acyl-carrier-protein] reductase	-3.58
HTH_0062	undecaprenyl-diphosphatase	-3.09
HTH_0068	4-hydroxy-3-methylbut-2-en-1-yl diphosphate synthase	-3.48
HTH_0202	long-chain-fatty-acid CoA ligase	-5.59
HTH_0203	putative thioesterase	-3.93
HTH_0966	sulfide dehydrogenase flavoprotein subunit	-304.36
HTH_1611	1-deoxy-D-xylulose 5-phosphate reductoisomerase	-8.01
[P] Inorganic ion transport and metabolism		
Locus tag	Description	Fold change (-[WT]/[dHdrA])
HTH_0048	ABC-type metal ion transport system permease component	-3.24
HTH_0160	nosD protein	-4.09

HTH_0469	phosphate uptake regulator	-7.82
HTH_0634	arsenite-transporting ATPase	-7.06
HTH_0932	superoxide dismutase [Cu-Zn]	-13.19
HTH_1402	metal ion ABC transporter permease	-4.60
HTH_1403	metal ion ABC transporter substrate-binding protein	-32.32
HTH_1509	heavy metal efflux pump, CzcA family	-10.10
HTH_1692	heavy metal efflux pump, CzcA family	-8.65
HTH_1710	ABC-type phosphate transport system permease protein	-6.51
HTH_1711	ABC-type phosphate transport system permease protein	-6.73
HTH_1712	ABC-type phosphate transport system ATP-binding protein	-5.22
HTH_1811	cation transporting ATPase, E1-E2 family	-21.46
HTH_1812	cation efflux system protein	-6.16
[Q] Secondary metabolites biosynthesis, transport, and catabolism		
Locus tag	Description	Fold change (-[WT]/[dHdrA])
HTH_1059	thioesterase family protein	-10.15
Poorly characterized		
[R] General function prediction only		
Locus tag	Description	Fold change (-[WT]/[dHdrA])
HTH_0147	predicted Fe-S oxidoreductases	-11.90
HTH_0148	hypothetical protein	-8.38
HTH_1060	aldo/keto reductase	-6.39
HTH_1489	hypothetical protein	-3.07
HTH_1786	beta-lactamase family protein	-4.41
HTH_1871	biotin synthase-related protein	-3.01
HTH_1875	hypothetical protein	-8.07
[S] Function unknown		
Locus tag	Description	Fold change (-[WT]/[dHdrA])
HTH_0132	hypothetical protein	-3.48

HTH_0445	predicted permease	-3.30
HTH_0654	conserved hypothetical protein	-4.90
HTH_1057	putative permease	-4.05
HTH_1506	hypothetical protein	-8.83
HTH_1888	hypothetical protein	-4.83
Others		
Locus tag	Description	Fold change (-[WT]/[dHdrA])
HTH_0011	hypothetical protein	-3.22
HTH_0026	permease of the major facilitator superfamily	-3.66
HTH_0027	permease of the major facilitator superfamily	-11.38
HTH_0093	hypothetical protein	-6.16
HTH_0102	hypothetical protein	-7.47
HTH_0146	NirF protein	-13.82
HTH_0149	NirN protein	-10.05
HTH_0237	hypothetical protein	-7.78
HTH_0270	hypothetical protein	-3.59
HTH_0282	hypothetical protein	-3.71
HTH_0283	nitric oxide reductase cytochrome b subunit	-30.80
HTH_0284	nitric oxide reductase cytochrome c subunit	-18.28
HTH_0350	hypothetical protein	-12.86
HTH_0351	hypothetical protein	-22.85
HTH_0394	hypothetical protein	-3.39
HTH_0429	hypothetical protein	-4.44
HTH_0516	hypothetical protein	-4.22
HTH_0517	phage recombination protein	-4.33
HTH_0518	hypothetical protein	-6.00
HTH_0519	hypothetical protein	-6.48
HTH_0520	hypothetical protein	-6.34
HTH_0521	hypothetical protein	-7.01
HTH_0522	hypothetical protein	-7.56
HTH_0527	hypothetical protein	-9.13
HTH_0528	hypothetical protein	-15.10
HTH_0529	hypothetical protein	-11.58

HTH_0531	hypothetical protein	-6.76
HTH_0533	hypothetical protein	-19.14
HTH_0534	hypothetical protein	-6.60
HTH_0542	hypothetical protein	-4.60
HTH_0543	phage uncharacterized protein	-13.43
HTH_0544	putative portal protein	-10.93
HTH_0545	hypothetical protein	-10.90
HTH_0546	hypothetical protein	-14.50
HTH_0547	hypothetical protein	-9.95
HTH_0548	putative phage major head protein	-15.38
HTH_0549	hypothetical protein	-24.94
HTH_0550	hypothetical protein	-22.57
HTH_0551	hypothetical protein	-15.40
HTH_0552	hypothetical protein	-6.34
HTH_0553	hypothetical protein	-7.50
HTH_0554	hypothetical protein	-5.94
HTH_0555	hypothetical protein	-7.30
HTH_0556	hypothetical protein	-6.51
HTH_0557	hypothetical protein	-9.32
HTH_0558	hypothetical protein	-9.72
HTH_0559	hypothetical protein	-7.18
HTH_0560	hypothetical protein	-7.21
HTH_0561	hypothetical protein	-5.99
HTH_0562	hypothetical protein	-8.24
HTH_0563	hypothetical protein	-8.06
HTH_0564	hypothetical protein	-3.84
HTH_0565	hypothetical protein	-13.72
HTH_0566	hypothetical protein	-23.14
HTH_0567	hypothetical protein	-17.82
HTH_0603	peptidoglycan associated lipoprotein	-3.60
HTH_0633	hypothetical protein	-22.06
HTH_0678	hypothetical protein	-6.98
HTH_0679	hypothetical protein	-10.06
HTH_0680	hypothetical protein	-16.06
HTH_0681	hypothetical protein	-9.55

HTH_0726	ribosomal protein L36	-4.55
HTH_0858	DNA-directed RNA polymerase beta subunit	-7.60
HTH_0889	hypothetical protein	-6.10
HTH_0890	hypothetical protein	-4.21
HTH_0891	phage tail tape measure protein	-7.60
HTH_0892	hypothetical protein	-7.27
HTH_0893	hypothetical protein	-5.33
HTH_0894	hypothetical protein	-4.57
HTH_0895	hypothetical protein	-4.18
HTH_0912	hypothetical protein	-6.85
HTH_0913	hypothetical protein	-5.43
HTH_0914	major structural phage protein	-4.16
HTH_0924	hypothetical protein	-4.41
HTH_0925	hypothetical protein	-3.14
HTH_0926	hypothetical protein	-3.78
HTH_0929	formate dehydrogenase alpha subunit	-27.22
HTH_0979	hypothetical protein	-3.40
HTH_1020	hypothetical protein	-74.74
HTH_1066	hypothetical protein	-4.02
HTH_1239	hypothetical protein	-25.90
HTH_1240	hypothetical protein	-15.24
HTH_1241	hypothetical protein	-14.75
HTH_1332	ubiquinol-cytochrome c reductase cytochrome c1 subunit	-4.06
HTH_1404	hypothetical protein	-47.79
HTH_1433	hypothetical protein	-3.38
HTH_1442	hypothetical protein	-3.92
HTH_1443	hypothetical protein	-4.90
HTH_1445	Tfp pilus assembly protein tip-associated adhesin PilY1-like precursor	-7.73
HTH_1446	hypothetical protein	-3.12
HTH_1499	tetratricopeptide repeat family protein	-4.29
HTH_1501	hypothetical protein	-73.02
HTH_1657	hypothetical protein	-3.61
HTH_1688	sensor histidine kinase	-7.31
HTH_1690	hypothetical protein	-47.56
HTH_1715	putative nitrate reductase subunit	-20.56

HTH_1717	nitrate reductase alpha subunit	-23.21
HTH_1784	hypothetical protein	-5.15
HTH_1806	efflux transporter	-6.24
HTH_1823	abortive infection protein	-4.04
HTH_1824	general secretion pathway protein K	-3.41
HTH_1876	hypothetical protein	-8.33
HTH_1880	hypothetical protein	-17.71
HTH_1908	fumarate reductase subunit C	-3.35